

2

AD-A265 032

PL-TR-93-2036



HIGH-LATITUDE ELECTRIC FIELD STUDIES USING DMSP DATA

M. R. Hairston
R. A. Heelis

University of Texas at Dallas
Center for Space Sciences
P.O. Box 830688, M/S FO22
Richardson, TX 75083-0688

18 February 1993

Final Report
1 December 1989—28 February 1993



Approved for public release: distribution unlimited

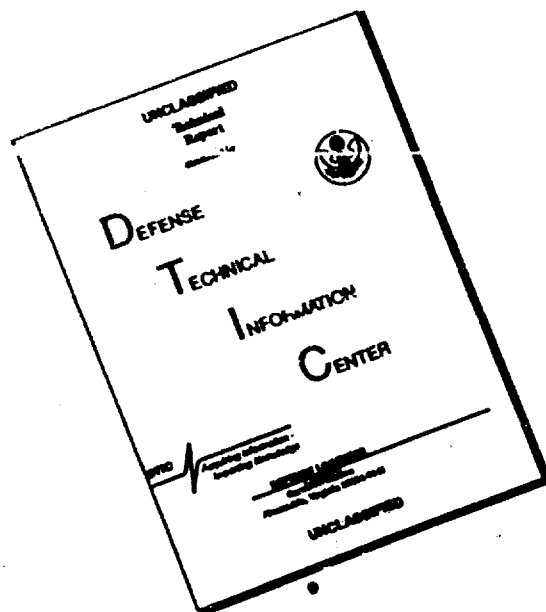


PHILLIPS LABORATORY
Directorate of Geophysics
AIR FORCE MATERIEL COMMAND
HANSCOM AIR FORCE BASE, MA 01731-3010

93-10679

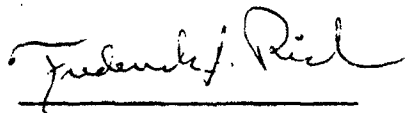
93-10679

DISCLAIMER NOTICE

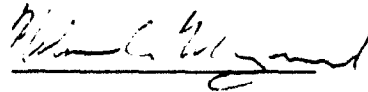


THIS DOCUMENT IS BEST QUALITY AVAILABLE. THE COPY FURNISHED TO DTIC CONTAINED A SIGNIFICANT NUMBER OF PAGES WHICH DO NOT REPRODUCE LEGIBLY.

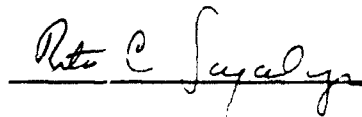
"This Technical report has been reviewed and is approved for publication"



FREDERICK J. RICH
Contract Manager



NELSON C. MAYNARD
Branch Chief



RITA C. SAGALYN
Division Director

This report has been reviewed by the ESD Public Affairs Office (PA) and is releasable to the National Technical Information Service (NTIS).

Qualified requestors may obtain additional copies from the Defense Technical Information Center. All others should apply to the National Technical Information Service.

If your address has changed, or if you wish to be removed from the mailing list, or if the addressee is no longer employed by your organization, please notify PL/TSI, Hanscom AFB, MA 01731. This will assist us in maintaining a current mailing list.

Do not return copies of this report unless contractual obligations or notices on a specific document requires that it be returned.

REPORT DOCUMENTATION PAGE			Form Approved OMB No 0704 0188	
Public reporting burden for this collection of information is estimated to average 1 hour per response, including the time for reviewing instructions, searching existing data sources, gathering and maintaining the data needed, and completing and reviewing the collection of information. Send comments regarding this burden estimate or any other aspect of this collection of information, including suggestions for reducing this burden, to Washington Headquarters Services, Directorate for Information Operations and Reports, 1215 Jefferson Davis Highway, Suite 1204, Arlington, VA 22202-4302, and to the Office of Management and Budget, Paperwork Reduction Project (0704-0188), Washington, DC 20503.				
1. AGENCY USE ONLY (leave blank)	2. REPORT DATE 18 February 1993	3. REPORT TYPE AND DATES COVERED Final (1 Dec 1989-28 Feb 1993)		
4. TITLE AND SUBTITLE High-Latitude Electric Field Studies Using DMSP Data		5. FUNDING NUMBERS PE 61102F PR 2311 TA 65 WE JA		
6. AUTHOR(S) M. R. Hairston R. A. Heelis		Contract F19628-90-K-0002		
7. PERFORMING ORGANIZATION NAME(S) AND ADDRESS(ES) University of Texas at Dallas Center for Space Sciences P.O. Box 830688, M/S F022 Richardson, TX 75083-0688		8. PERFORMING ORGANIZATION REPORT NUMBER		
9. SPONSORING/MONITORING AGENCY NAME(S) AND ADDRESS(ES) Phillips Laboratory 29 Randolph Road Hanscom AFB, MA 01731-3010 Contract Manager: Frederick Rich/GPSC		10. SPONSORING/MONITORING AGENCY REPORT NUMBER PL-TR-93-2036		
11. SUPPLEMENTARY NOTES				
BEST AVAILABLE COPY				
12a. DISTRIBUTION/AVAILABILITY STATEMENT Approved for public release; distribution unlimited		12b. DISTRIBUTION CODE		
13. ABSTRACT (Maximum 200 words) Analysis using data from the ion drift meter in the SSIES instrument package on the DMSP series of satellites is used to calculate the electrostatic potential distribution in the polar ionosphere. Numerous geophysical parameters such as the location and magnitude of the potential extreme and the classification of the potential distribution as one of the three Heppner-Maynard models can be derived from this data analysis. An earlier version of this analysis procedure (DMSPOTMOD) is described. This procedure has been expanded into a series of programs under the name DMSPDBASE which generate a database of the ionospheric parameters and results from this analysis. These calculated parameters serve as necessary inputs to the MSFM (Magnetospheric Specification and Forecast Model) used by the Air Weather Service. This report describes each version of the series up to the final version DMSPDBASE4 along with a description of the formats used for the database. New algorithms have been added to the routine in order to improve the selection routine for the endpoints, generalize the Heppner-Maynard model classification algorithm so that it will accommodate any orientation of the satellite track, calculate the true cross polar cap potential drop from the observed potential drop, etc. Analysis results into characterizing the overall potential distribution in both				
14. SUBJECT TERMS DMSP; ionosphere; ionospheric plasma; ionospheric plasma convection pattern; spacecraft data analysis		15. NUMBER OF PAGES 50		16. PRICE CODE
17. SECURITY CLASSIFICATION OF REPORT Unclassified	18. SECURITY CLASSIFICATION OF THIS PAGE Unclassified	19. SECURITY CLASSIFICATION OF ABSTRACT Unclassified	20. LIMITATION OF ABSTRACT SAR	

CONT OF BLOCK 13:

hemispheres during time of southward IMF and analysis of the evolution of the potential distribution during times of northward IMF are presented. Various collaborations with other users incorporating DMSP data are listed along with presentations and publications which have come from this work.

Table of Contents

1. INTRODUCTION	1
2. DMSPOTMOD	1
3. DMSPDBASE AND SUBSEQUENT UPGRADES	3
3.1 DMSPDBASE1 – Building the Database	3
3.2 DMSPDBASE1B – Upgrading the Endpoint Selection Routine	7
3.3 DMSPDBASE2 – Modifying the Highest Latitude Passes	7
3.4 DMSPDBASE3 – Correcting for the “H+ fuzz”	11
3.5 DMSPDBASE4 – Upgrading the Heppner–Maynard Model Identification and Further Corrections to the Endpoint Selection Routine	20
4. OTHER ANALYSIS EFFORTS	39
5. REFERENCES	45

FORM 3110 1-78 (REV. 10-1977) 5

Accession For	
NTIS GRAB	<input checked="" type="checkbox"/>
DTIC TAB	<input type="checkbox"/>
Unannounced	<input type="checkbox"/>
Justification	
By _____	
Distribution/for _____	
Availability Codes	

A-1

1. INTRODUCTION

Over the past three years we have tried to increase the effectiveness of the data interpretation from the DMSP SSIES instrumentation. We have pursued two major paths to this goal. One is the development and refinement of algorithms for producing the geophysical parameters and another is the examination of data ensuring that the algorithms capitalize on the state of our knowledge about the ionospheric processes being described.

The following report describes the software development tasks undertaken to make the data reduction software more robust. These include adaptations to changing ion composition along the spacecraft track and to changes in the high latitude convection pattern resulting from magnetic activity. We have also adapted algorithms for identifying the large scale features in the ionospheric convection pattern from a single satellite pass through the pattern. In addition to the algorithm development and refinement, we have also started to identify reproducible features in the high latitude motion that exist when the interplanetary magnetic field is directed northward. We expect that by associating measured quantities with specific behavior in the plasma motion we will be able to develop a characterization of the flow that is comparable in quality to that presently available during southward IMF. The following sections document the work performed in more detail.

2. DMSPOTMOD

DMSP Potential Model or DMSPOTMOD, which was delivered at the end of 1989 with support from a previous contract, was the first major analysis program used for classifying the high latitude environment based on SSIES data. Much of the work during the past three year period has been in exploiting and upgrading the analysis developed for DMSPOTMOD. This section gives an overview of the scope and purpose of DMSPOTMOD. Further details are given by Heelis and Hairston [1990].

The Defense Meteorological Satellite Program (DMSP) is a series of polar orbiting satellites designed to observe the weather on Earth and to monitor the near-Earth space environment at 840 km. The Special Sensor—Ions, Electrons and Scintillation (SSIES) package which has flown on all DMSP satellites since F8 was launched in summer 1987, provides a measure of the velocity, density, tempera-

ture, and chemical composition of the thermal plasma in the upper ionosphere. One of the instruments on SSIES is the Ion Drift Meter (IDM) which faces into the direction of the satellite velocity and measures the vertical and horizontal components of the ion flow perpendicular to the satellite velocity. Each velocity component is sampled six times a second. Taking the perpendicular flow of the ions (v) and the magnetic field at the satellite (B), the electric field parallel to the satellite's velocity vector (E) can be calculated using the equation

$$E = -v \times B.$$

Integrating the electric field along the satellite track provides a measure of the electrostatic potential along the track.

In general, the flows and potentials are small everywhere along the satellite orbit except in the polar regions. Here potential differences on the order of tens of kilovolts exist across the polar region. The magnitude and distribution of this potential are important parameters for understanding the ionospheric environment. Most notably here, these parameters are important inputs to the Magnetospheric Specification and Forecast Model (MSFM) developed by Rice University for use by the Air Weather Service. DMSPOTMOD is a program that can take the ion flow data from the DMSP SSIES package and produce a measurement of the polar cap potential that can be used by the MSFM.

Data for one half orbit going from an equatorial crossing to the next equatorial crossing are averaged into four-second bins. The horizontal flow data are corrected to remove the effect of corotation. The baselines of both components of the flow are established by minimizing the flow near 50 degrees magnetic latitude. The 50 degree magnetic latitude is assumed to be at zero potential, and thus under steady state condition the potential should be zero at both points where the spacecraft crosses this latitude. However, this rarely occurs either because there are some changes in the potential distribution during the twenty minutes it takes the satellite to traverse the polar region or because there exist systematic offsets in the measured velocity. For most polar passes an offset in potential remains in the calculated potential distribution when the spacecraft recrosses the 50 degree magnetic latitude. A corrected potential distribution which has both ends at zero potential is generated by taking the value of this offset and doing a linear correction to the measured potential. This corrected potential distribu-

tion is used to determine the magnitude and locations of the maximum and minimum potential seen along this pass, as well as the location of the zero potential point between the maximum and minimum. The geographic asymmetry of the location of the zero point (i.e.—the relative distance from the zero point to the location of the maximum and minimum) is used to designate which of the three Heppner–Maynard patterns (Heppner and Maynard, 1987) best fits this pass. The level of noise in the flow data inside the polar cap is used to determine a quality flag for the data for this pass and the highest magnetic latitude reached by the satellite is used to determine a correction factor to be applied to the observed potential maximum and minimum. Finally, these parameters along with a unique identification number for the pass (SFINDEX) are saved in a data file called MSMDATA.DAT.

3. DMSPPDBASE AND SUBSEQUENT UPGRADES

After DMSPPOTMOD was delivered to Geophysics Lab, the program was upgraded in spring 1990 to run successive passes and save the data in a database format. This new version was renamed DMSPPDBASE1 and delivered in early summer 1990. Since then there have been four revisions to the program with the latest, DMSPPDBASE4, being delivered in January 1993 with this report. Each revision improved on the quality of the data analysis of its predecessor and was based on our increased understanding of the data. We shall examine each of these upgrades and its results in turn.

3.1 DMSPPDBASE1—Building the Database

In the original DMSPPOTMOD program the values for the ion flow velocity averages, their standard deviations, the potentials, and the satellite's locations were calculated for each four–second timestep during a polar pass. These data were necessary to calculate the overall potential distribution during a pass and to determine the parameters that were saved in the MSMDATA.DAT data file, but *once these parameters were found, the four–second data were discarded.* With increased data handling capability at both UT–Dallas and at Phillips Laboratory/GP, this four–second data could also be saved for the database. DMSPPDBASE1 adapted the DMSPPOTMOD program so that it could read an entire magnetic tape containing ten days of telemetry data in the Time–History–Database format. As it processed the data on a polar pass by polar pass basis, it would write the data into two files which are referred to as the “shortfile” (DMSPPPARAM.DAT) and the “longfile” (DMSPPOT-

BIN.DAT). The shortfile contained only the key parameters (potential maximum and its location, zero crossing location, model number, etc.) for each pass and was identical to the MSMDATA file generated by DMSPPOTMOD. The longfile contains the geophysical data about the IMF and K_p indices before, during, and after the pass followed by the measured flow data and calculated potential data for each four-second period covering half an orbit from equatorial crossing to equatorial crossing. The longfile was created as an unformatted sequential file.

The format for the longfile is given in the following tables. The first table gives the format for the first line of each longfile.

PARAMETER	VARIABLE NAME	DESCRIPTION
index number for pass	SFINDEX	unique index number for this polar pass, format based on satellite number, year, day of year, hour, and minute when this pass started at the equator (NNYYDDDDHHMM)
IMF B_x component	BXPREV	these are the hourly averaged IMF components during the hour PRIOR to start of pass
IMF B_y component	BYPREV	
IMF B_z component	BZPREV	
IMF B_x component	BXSTRT	these are the hourly averaged IMF components during the hour AT the start of the pass
IMF B_y component	BYSTRT	
IMF B_z component	BZSTRT	
IMF B_x component	BXSTOP	these are the hourly averaged IMF components during the hour AFTER the start of pass (Note that all the IMF values are given in nanoteslas in the geocentric solar magnetic (GSM) coordinate system)
IMF B_y component	BYSTOP	
IMF B_z component	BZSTOP	
AE index at start of pass	IAEINDEX1	not yet available, fill data
AE index at end of pass	IAEINDEX2	not yet available, fill data
K_p index at start of pass	KPSTART	K_p index is coded as a 2-digit integer as follows: $K_p 0 = 0$, $K_p 0+ = 1$, $K_p 1- = 2$, $K_p 1 = 3$, $K_p 1+ = 4$, ..., $K_p 9- = 26$, $K_p 9 = 27$
K_p index at end of pass	KPSTOP	
number of 4-second data blocks	IMAX	always equal to 810, or 54 minutes of data, serves as a check on the size of the file

horizontal flow correction	CHF	offset applied to the horizontal and vertical flow data in order to bring the endpoints to zero velocity
vertical flow correction	CVF	

(Note that for a given pass, the SFINDEX number of the longfile is the same as the SFINDEX number of the shortfile for that pass. This allows for easy correlation of passes between files in the two databases. For the hourly averaged B_x , B_y , and B_z components of the IMF, note that in this analysis, the hour in which the pass begins is defined as the hour when the satellite crossed the equator, even if that occurs during the 59th minute of that hour. If there are no IMF data available for any of these times, then fill values of 999 are saved in their place to the file. The rationale for recording this IMF data is to allow a search of the database for passes which occurred during times when the IMF was steady over a period of two or three hours. As the AE indices are not yet available, fill data of 990 is saved to the file. At some point in the future when this data becomes available, it will be incorporated into the database. The number of four-second blocks in this pass is given as the value of IMAX. This is always equal to 810, corresponding to 54 minutes worth of data. Originally the number of four-second blocks for each pass was going to vary depending on exactly the time between the equatorial crossings, thus causing IMAX to vary. It was decided to make all the passes a uniform length to simplify the processing and the IMAX value was retained as a check on this. A length of 54 minutes takes each of the satellites from an equatorial crossing to slightly past the next equatorial crossing. This results in some overlap of data in the files, but this is preferable to the possibility of missing some data by choosing too short a time length. The final values in the are the values for the horizontal flow correction and the vertical flow correction which were applied to the de-rotated flow data to bring the endpoints of the flows for this pass to zero (CHF, CVF). These are saved for later work in checking for systematic variations in the drift of the baseline of the flow data.)

The next table gives the format for the remaining 810 lines of data in a longfile:

PARAMETER	VARIABLE	DESCRIPTION
time	XUTIME	given in seconds (0-86400)
horizontal ion flow velocity	FLWH3	four second averages given in kilometers/second (plus 3 km/s, see note below)
vertical ion flow velocity	FLWV3	

standard deviation of horizontal ion flow velocity	STDEVH	standard deviation of the data points included in the four second averages
standard deviation of vertical ion flow velocity	STDEVV	
number of points	NMBPTS	number of points included in the four second averages, nominally equal to 24, the number is the same for both horizontal and vertical analysis
electrostatic potential	POTLNG	corrected potential given in kilovolts
magnetic latitude (at satellite)	SCCHMLATS	given in degrees
magnetic latitude (at 110 km)	SCCHMLAT	given in degrees
magnetic local time (at 110 km)	SCCHMLTM	given in hours and decimal fractions of an hour
invariant latitude	SCCHINVLAT	given in degrees
geographic latitude	SCCHLAT	given in degrees
geographic east longitude	SCCHLONG	given in degrees

(The values for the ion flow velocities have had the corotation of the ionosphere and the flow offset values (CHF, CVF) removed, and thus are given in the inertial frame of reference fixed to the sun - Earth line. In order to conserve the space a negative sign would occupy in the record, all the values for the flow data have 3.0 km/s added to them before they are saved to the data file. This insures that all the flow values are positive. This excess is always removed when the data is read out. The standard deviation and number of points in the analysis are saved as a check on the noisiness and completeness of the data incorporated into the four-second flow averages. The values for the electrostatic potential are those of the corrected potential distribution described above. The geophysical coordinates every four seconds are interpolated using the one minute increments taken from the orbit data in the telemetry.)

The blocks of data for each pass are written sequentially onto the file until the full ten days of data have been analyzed. The writing of this data to the longfile occurs in BLOCK 4B of DMSPDBASE1. However, if the pass is determined to be unusable for some reason, then a null file of zeroes is written to the shortfile under the SFINDEX number for that pass, but no corresponding longfile is created.

3.2 DMSPDBASE1B—Upgrading the Endpoint Selection Routine

The first revision came later in summer of 1990. As a result of examining the data from the database, it became apparent that the algorithm for choosing the location of the endpoints of the pass should be improved. The original algorithm placed the endpoints symmetrically about the center of the magnetic coordinate system. Thus both ends would be at the same magnetic latitude. In the original algorithm both ends would be checked at 50 degrees magnetic latitude. If either point was unsuitable, then the algorithm checked both ends at 45 degrees magnetic latitude. This process repeated until suitable endpoints were found or the search terminated at 20 degrees magnetic latitude. While this worked for the majority of the cases, sometimes passes were encountered in which, for example, the starting endpoint at 50 degree magnetic latitude would be acceptable while the stopping endpoint was not. The program would check at 45 degrees magnetic latitude and then find the new starting point was unsuitable, but the new stopping endpoint was acceptable. In such a case the obvious solution would be to use the starting endpoint at 50 degrees and the stopping endpoint at 45 degrees. Instead the original algorithm would move on to the 40 degree endpoints and check those points. At best, both those points would be chosen, giving the pass an excess "tail" on either end, or, as happened in some cases, no case was found where both endpoints at the same latitude were suitable. This resulted in a usable pass being ruled as unsuitable and discarded from the database.

The modification was fairly simple. Block 2A was rewritten such that the search routine considered each endpoint separately. If the starting endpoint at 50 degrees was suitable but the stopping endpoint was not, then the program only continued searching for a suitable stopping endpoint. Once that was found, then the rest of the analysis on the pass continued.

3.3 DMSPDBASE2—Modifying the Highest Latitude Passes

As more passes were processed it was realized that errors in determining the ground track of the satellite in a magnetic coordinate system were occurring frequently during the passes that went above 80 degrees magnetic latitude. The two problems addressed here were an error in interpolating the four-second increments of the spacecraft's location in magnetic coordinates and an error in deter-

mining the magnetic latitude above 85 degrees. Both these problems were fixed in spring 1991 and the updated version after this was renamed DMSPDBASE2.

In the original DMSPDBASE1 program the four-second increments of magnetic latitude, magnetic local time, invariant latitude, geographic latitude and geographic longitude were determined by a simple linear interpolation of the values given every minute in the orbit data. This worked satisfactorily in most cases, but failed at latitudes higher than 80 degrees. The failure arises from treating polar coordinates as if they were rectilinear coordinates in the interpolation and simply interpolating each component individually. At lower latitudes where there was not much change in the magnetic local time in the one-minute intervals, thus very little error resulted from using such a method. But at the highest latitudes where there was a fairly large change in the magnetic local time over the course of one minute, this caused "scallop-shaped" curves to appear in the satellite's track (Figure 1). This was corrected by changing the interpolation procedure in the COROTFIX subroutine where the four-second increments were calculated and renaming the subroutine COROTFIXG. In the new interpolation procedure, the polar coordinates are transformed into rectilinear coordinates and then a linear interpolation is performed on them in order to obtain the four-second increments. After this, the new rectilinear coordinates of the four-second increments are transformed back into the original polar coordinate system, thus giving a straight ground track in the polar coordinate system.

The second problem occurred only when the satellite went above 85 degrees magnetic latitude. Magnetic latitude is computed by tracing the field line passing through the satellite down to 110 km and measuring the angle between that point and the magnetic dipole. The model used to determine the magnetic latitude for the orbit data in the DMSP header tended to have large errors in the calculations the closer the magnetic latitude got to 90 degrees. Thus on some passes that got close to the magnetic pole, the one-minute locations in the magnetic coordinate system showed an erroneously jagged path (Figure 2a) where one to three locations are pushed away from the true ground track.

This problem was solved by adding Block 1D to the program which takes any pass that goes above 85 degrees magnetic latitude and relocates the point(s) above 85 degrees using a third order polynomial least squares fit to the points surrounding it. While not all passes which went above 85 degrees

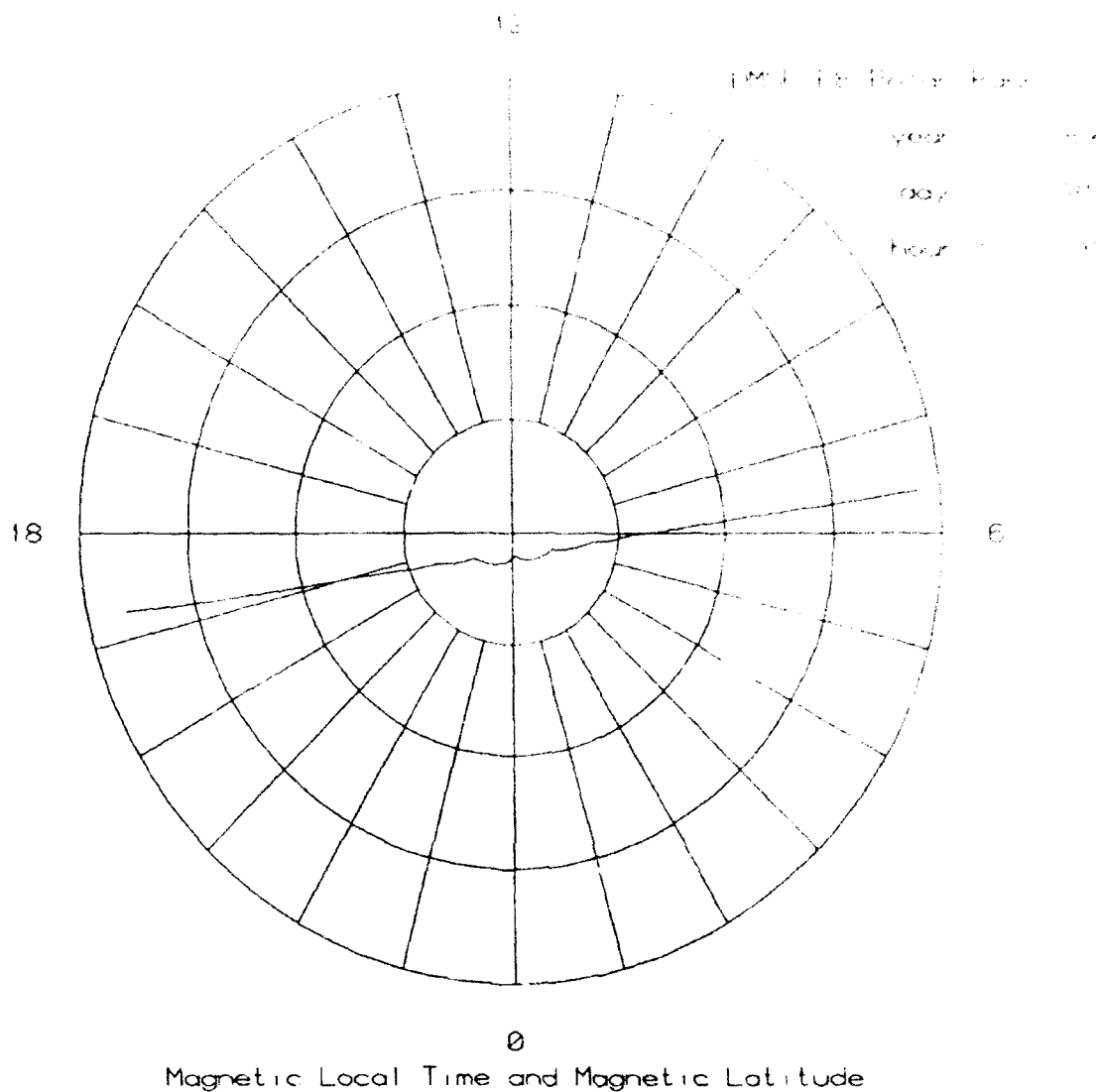


Figure 1. This plot shows the ground track of a DMSP-F8 polar pass in magnetic latitude and magnetic local time coordinates using the incorrect path interpolation from the original DMSPPOT-MOD routine. Note the small "scallop"-shaped humps near the poles that result from this interpolation. The cusps between the "scallops" are the locations of the one minute marks in the telemetry header. Note also that at lower latitudes, this interpolation works quite well.

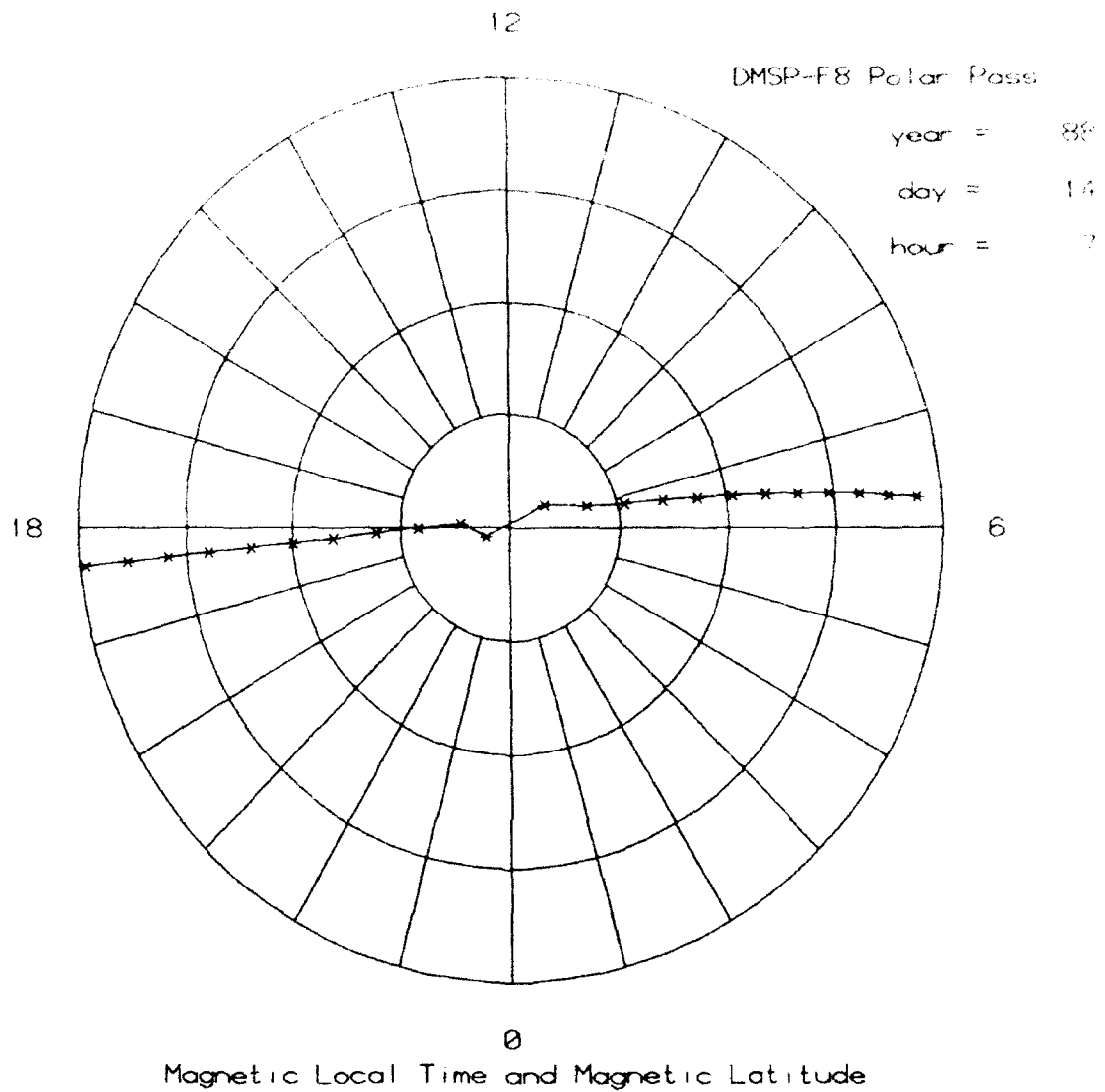


Figure 2a. This polar dial shows an example of a high latitude pass with a single point out of alignment. The asterisks denote the locations of the satellite at the one minute marks given in the telemetry header.

had the high latitude point mislocated, the error occurred frequently enough that it was deemed worthwhile to apply the routine automatically to all of them. The rationale for this was that if the highest latitude point was not mislocated, then the smoothing routine had very little effect on it.

The smoothing was done by taking the locations in magnetic latitude and magnetic local time of the seven points at the highest magnetic latitude and converting them into a rectilinear coordinate system. The seven x components and the seven y components along with their corresponding times are independently run through a least squares subroutine (LESSQ3) which returns a set of coefficients for a third-order polynomial. The program calculates a new set of x and y coordinates for the seven locations. This gives a corrected location for the erroneous point above 85 degrees with only a minimum adjustment to the locations of the surrounding points (Figure 2b). The locations for the new points are then transformed back into magnetic latitude/magnetic local time coordinates and replace the original values for of magnetic latitude and magnetic local time in the arrays SCMLAT and SCMLT. Note that this correction is done before the program calls the COROTFIXG subroutine and thus the interpolated four-second increments of magnetic latitude and magnetic local time are based on these smoothed values, not the original erroneous ones.

3.4 DMSPDBASE3—Correcting for the “H+ fuzz”

Initially the algorithm we designed to perform the potential analysis assumed that the vertical and horizontal ion drift were close to zero in the region equatorward of the auroral zone. (In most cases the 50 degree magnetic latitude points are chosen as the starting and stopping point and the flow data are close to zero there. The algorithm does allow for other points to be chosen if the polar cap region has expanded, as in the case of the “Great Storm” of March 1989.) The baseline for the entire pass is then zeroed using the average value of these endpoints and the analysis is performed on the corrected flow data. During the period of December 1987 through March 1988 an anomaly appeared in the data of DMSP-F8; both the horizontal and vertical flow data showed large values (> 0.9 km/s) and a large scatter (~ 0.4 km/s) during the northbound leg of the orbit at MLT 0600. These “humps” in the data began at midlatitudes in the southern hemisphere and continued until just before the satellite reached the northern auroral region (Figure 3). The “humps” were named “H+ fuzz” and analy-

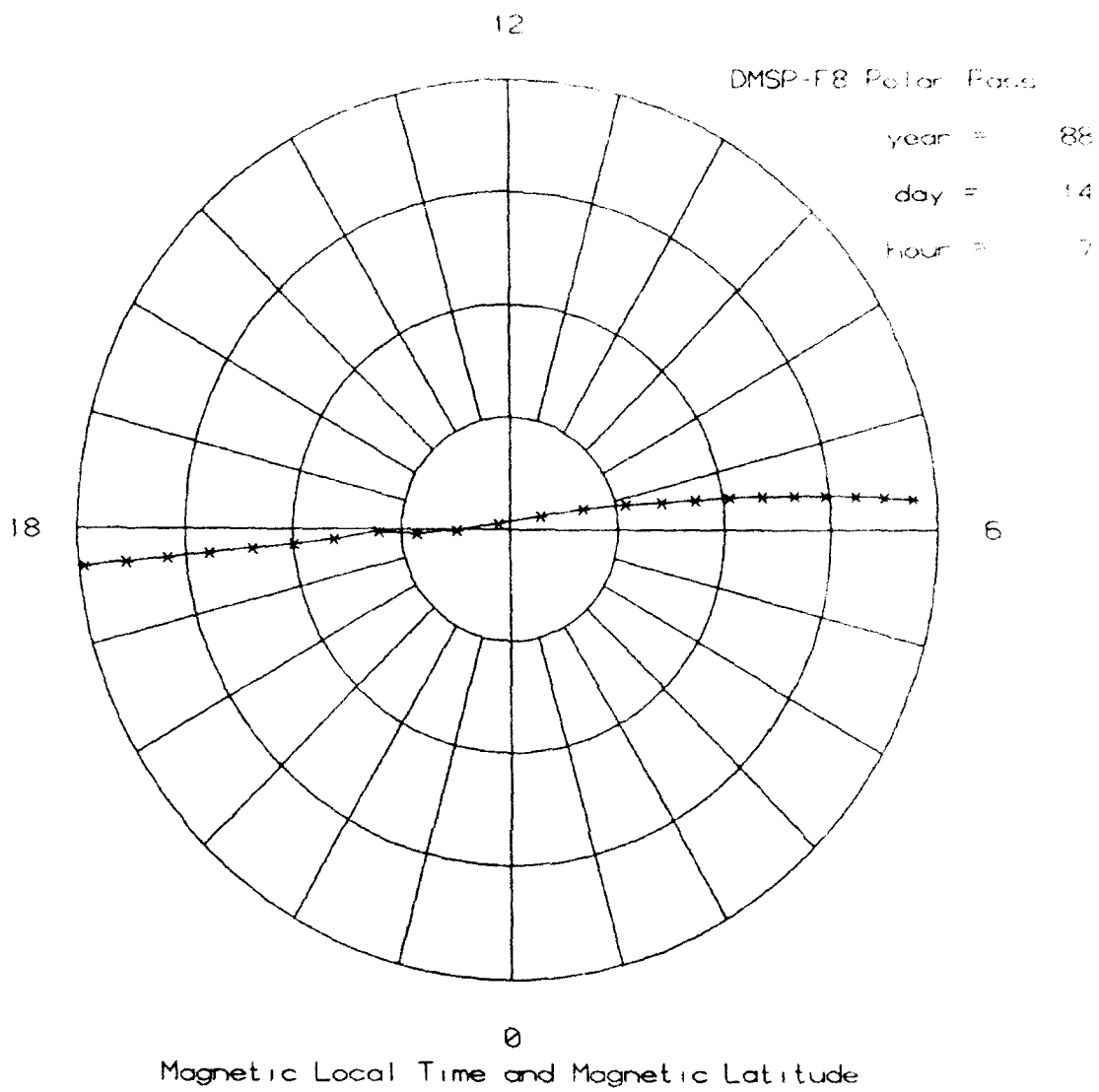


Figure 2b. This polar dial shows the same polar pass shown in figure 2a after the smoothing algorithm has been applied to the misaligned point and the six points surrounding it.

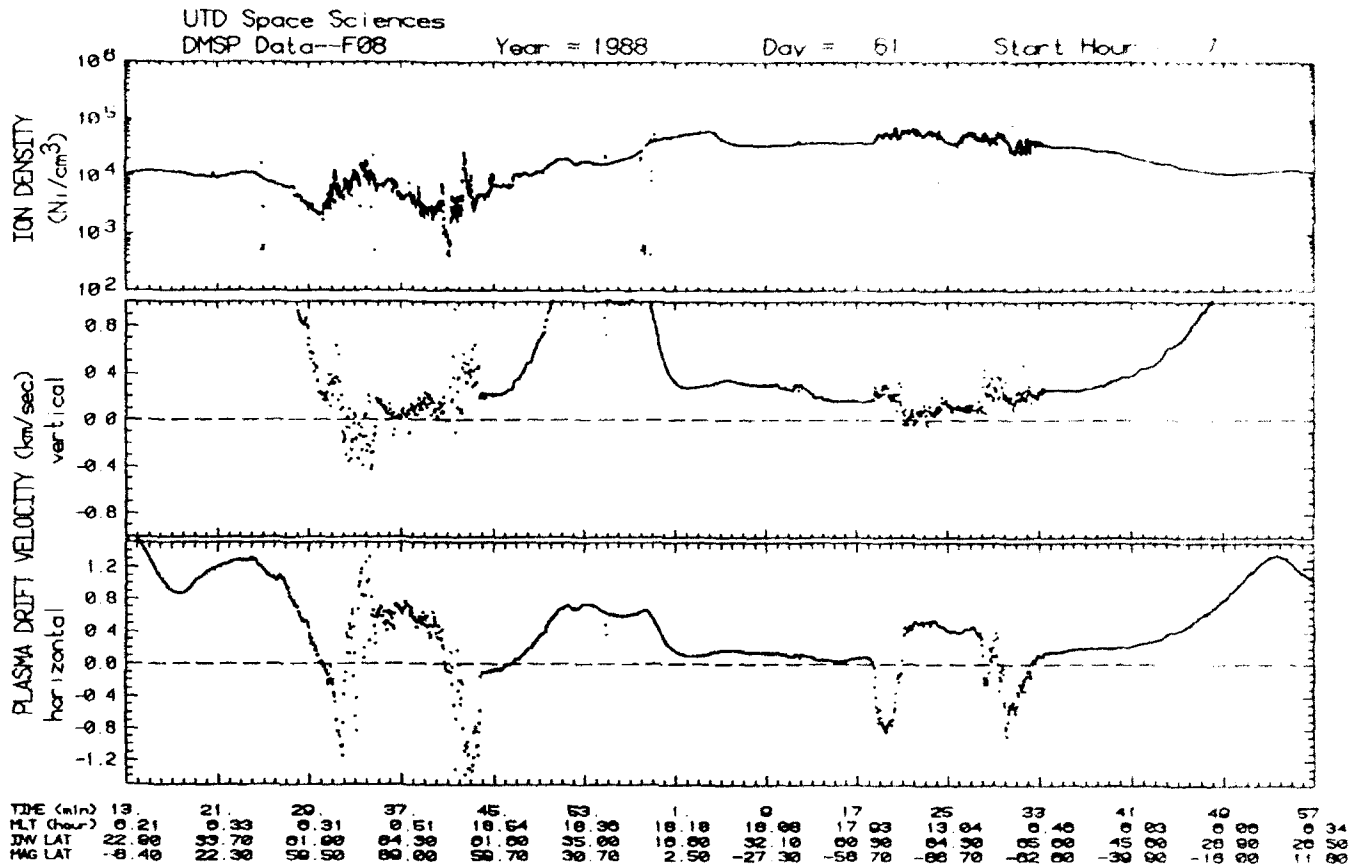


Figure 3. This plot shows the number density and plasma flow data for a single orbit of ES on 1 March 1988. The plots starts as the satellite crosses the equator heading northward, goes over the northern polar region, past the equator at the midpoint of the plot, over the southern polar region, and ends at the next northbound equator crossing. The H⁺ fuzz is apparent as the non-zero velocities in both the horizontal and vertical flows on either side of the northern polar region. Nominally the flow velocities in those regions should be close to zero such as are seen surrounding the southern polar regions.

sis showed that they were an artifact of the IDM whenever the light ions (hydrogen and helium ions) concentration was greater than 20 or 25% of the total ion density. This is consistent with the conditions seen in the polar ionosphere during that hemisphere's winter, particularly on the nightside. Since the F8 orbit is tilted at 98.8 degrees, it is always on the nightside of the 0600–1800 hours local time line in the northern hemisphere and on the dayside of the same line in the southern hemisphere. This explains why this phenomenon was not observed in the southern hemisphere when F8 was first launched in June 1987 during the southern winter. Instead it first appeared only in the northern hemisphere in the late fall of 1987. The H⁺ fuzz did not appear on the southbound leg of the northern hemisphere orbit because that occurred in the early evening portion of the ionosphere at MLT 1800. The plasma there had just moved in from the dayside and was still hot enough that the scale height of the O⁺ ions was large and the relative abundance of O⁺ at 800 km was > 75–80%. As this plasma moved around into the nightside, it cooled off and the scale height decreased. By the time the plasma had moved around to 0600 MLT many of the heavier O⁺ ions had sunk to lower altitudes leaving the lighter H⁺ and He⁺ ions to make up a larger proportion of the plasma at 800 km. This explains why the H⁺ fuzz was so much smaller on the northern duskside which had just recently entered darkness. In the southern hemisphere no fuzz was seen on the duskside leg of the orbit because that portion was still sunlit. On the southern dawnside the H⁺ fuzz would appear at midlatitudes because this plasma had only recently moved into the sunlit region.

Curiously, the phenomenon of the H⁺ fuzz did not reappear in the next winter period (December 1988–March 1989) nor in any of the subsequent winter periods through March 1992 in the F8 data. We believe this to be caused by the increased solar activity which began in 1988. During solar maximum the atmosphere is hotter than during solar minimum and in turn the scale heights of the various species in the plasma are larger, thus keeping the proportion of O⁺ at 800 kilometers above the 75–80% level. While we do not expect this H⁺ anomaly to reappear before the end of F8's operational lifetime, it may appear in the F11 (and subsequent satellites in the 0400–1600 MLT orientation) data in the next few years.

The H+ fuzz is a concern because the original algorithm used in DMSPOTMOD and DMSP-DBASE tended to choose starting points inside the H+ fuzz region for passes in the northern hemisphere. This resulted in an incorrect baseline being set, which in turn produced bad results for the calculated potential. The algorithm in DMSPDBASE was upgraded in the fall of 1991 so that it would avoid choosing starting points inside the H+ fuzz regions. Figures 4a and b show the same pass before and after the upgrade of this algorithm in Block 2A.

As shown in these figures, many passes show the H+ fuzz extended above the 50 degrees magnetic latitude on the dawn side. For this reason the new algorithm starts looking for a suitable starting endpoint at 65 degrees magnetic latitude. The criteria for choosing a suitable endpoint was determined empirically by examining the F8 flow data during the period from December 1987 through March 1988. A new subroutine named SEARCH was incorporated into the program which used the following procedure for determining whether a trial point at a given latitude is a suitable endpoint:

- 1) It checks the standard deviation for the four-second horizontal flow average (STDEVH) and the four-second vertical flow average (STDEVV) as well as the standard deviation of the averages for each component on either side of this trial point. If any one of these six standard deviations is greater than 0.14, then the data at this location is deemed to be too noisy to be suitable as an endpoint.
- 2) It checks how far the averaged flow values at this trial point deviate from zero. For most of the time for all the DMSP satellites the horizontal flow should be within ± 0.2 km/s of zero and the vertical flow should be within ± 0.35 km/s of zero. However there was a large offset in the flow baseline in the early months of F8, so for the 1987 period values of ± 0.4 km/s for the horizontal flow and ± 0.55 km/s for the vertical flow are used. If either the horizontal flow or vertical flow at this location is outside these limits, then this point is deemed unsuitable as an endpoint. This removes the chance that a point on the "hump" of the H+ fuzz region would be selected as an endpoint.

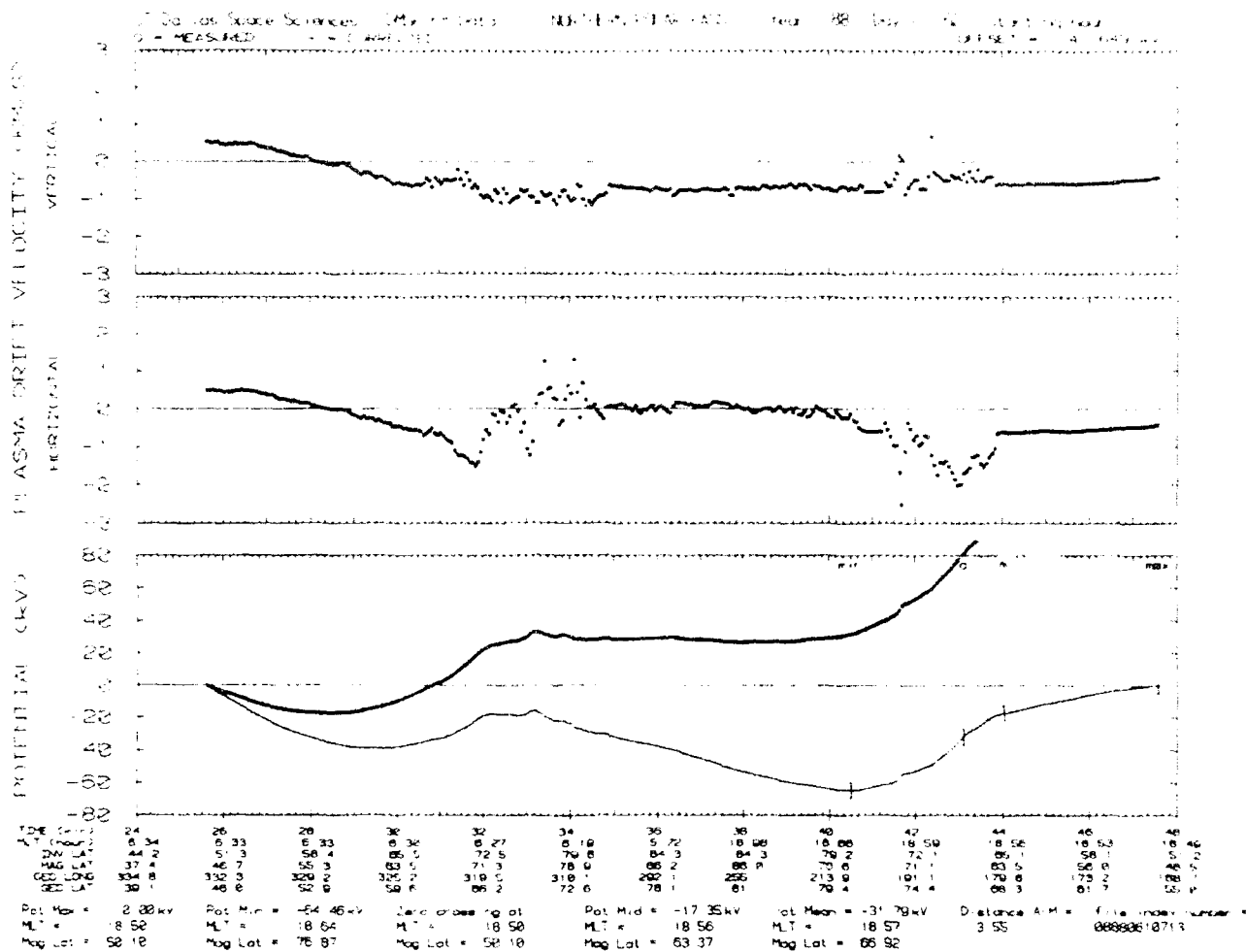


Figure 4a. This plot shows the analysis of the electrostatic potential for the northern polar pass shown in figure 3 without using the corrections incorporated into DMSPDBASE3. The program erroneously chose the 45 degree magnetic latitude point on the dawnside which is inside the H+ fuzz region (note the change in scales for the flow velocities between figures 3 and 4a). The difference between the flow velocities at the starting and stopping points are about 1 kilometer/second, thus the program takes the average of the two ends and sets a flawed baseline for the analysis. This results in the potential curve having a spurious negative potential portion between 45 and 60 degrees on the dawnside which wrecks the overall shape of the potential curve.

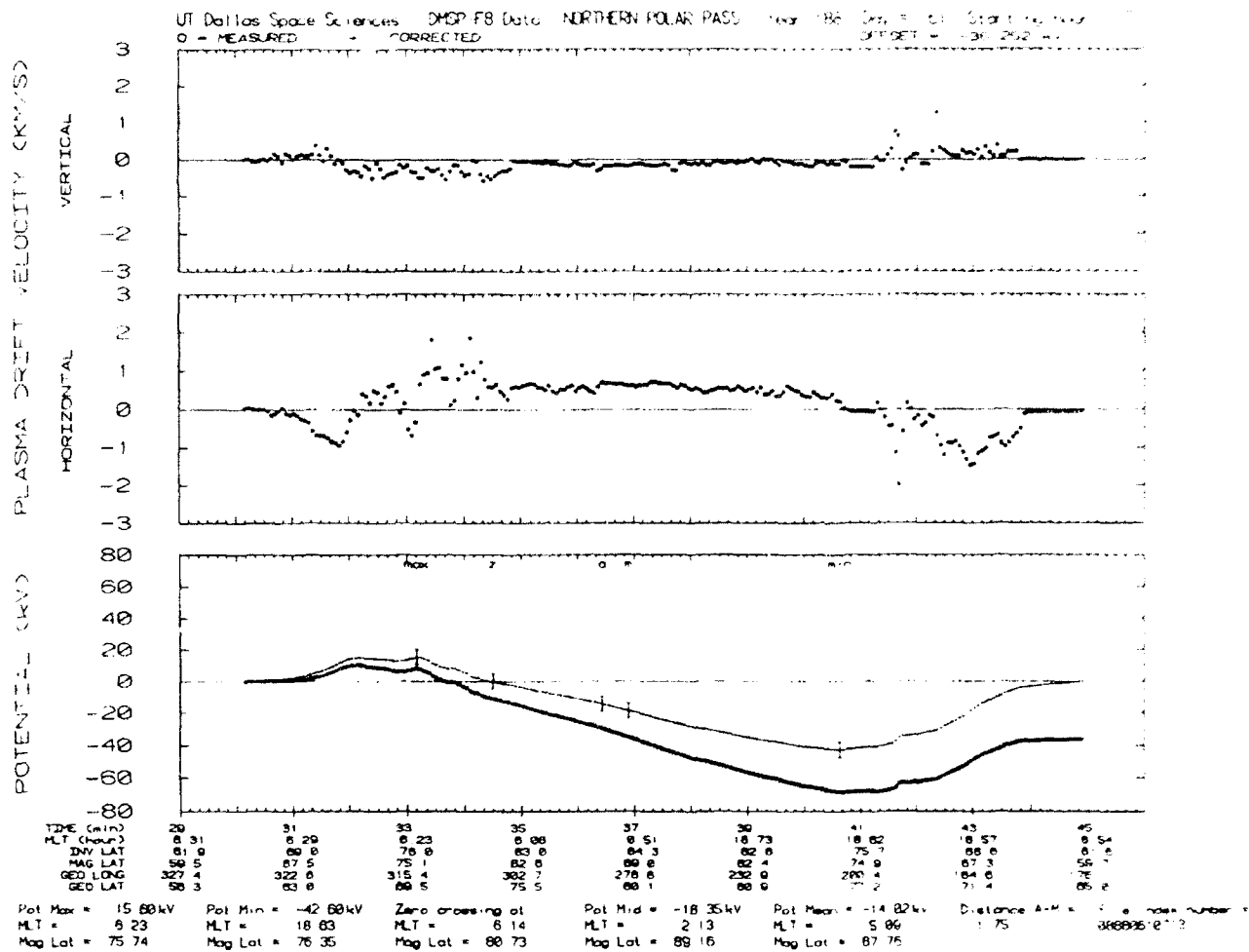


Figure 4b. This plot shows the same pass as figure 4a analyzed using the new algorithms in DMSPDBASE3. The new version of the analysis correctly selects usable endpoints at 62 and 60 degrees magnetic latitude, which results in an accurate calculation of the potential curve.

3) It takes the average of the trial point along with the two four-second averaged flow values prior to and two averages following the trial point. It calculates the variance for these five values and checks if it is greater than 0.006. This procedure is repeated for vertical flow values around the trial point. If either of these variances is greater than 0.006, then the region around this point has too much scatter and is deemed unsuitable for an endpoint. This check guards against choosing an endpoint in the H+ fuzz region where there is a large scatter in the four-second averaged flow data.

If all three of these checks are passed, then the SEARCH subroutine returns a value of 1 for the variable IGO to indicate that this point is suitable as an endpoint. The selection of the exact values of the cutoffs in the three checks in SEARCH was performed empirically to eliminate the chance of accidentally choosing an endpoint in the H+ fuzz region. These values may be changed to provide a looser or tighter selection criteria.

The endpoint algorithm in Block 2A was revised to change the order of the search for endpoints. The revised routine begins by checking the trial starting points at 65, 60, 55, and 50 degrees. If any of these were suitable, the suitable point lowest in latitude is picked as the starting point. If none of the four are suitable, the algorithm continues to inspect trial points at five degree increments until either a suitable starting point was found or the algorithm reaches 20 degrees latitude. If no suitable starting point has been reached by 20 degrees, the program starts the search again at 64 degrees and examines trial points in one degree increments. This continues until either a suitable starting point is found or it reaches 20 degrees latitude. If the algorithm fails to find a suitable starting point, the program branches to where it writes a null file for this pass to the shortfile in the database, then cycles back to start on the next pass. If the routine does find a suitable starting point, it repeats the same procedure to find a suitable stopping point. Doing the search in one degree increments will find a suitable endpoint for most cases, but it is a time-consuming procedure if attempted on the majority of non-H+ fuzz cases. Thus the rationale behind this algorithm is to try to five degree increment search first on all cases, only attempting the one degree increment search on those that failed.

The improvement of the new algorithm in DMSPDBASE3 is shown by comparing the results of the earlier version to the revised version for a typical period when the H+ fuzz appeared. For the period of March 1 through 10, 1988 DMSP-F8 data has 134 complete northern passes and 133 southern passes, these being defined as periods of uninterrupted data from equator crossing to next equator crossing. There is a data gap of about five orbits during the latter half of day 65 through the beginning of day 66. Those lost passes are not included in the totals below. For this comparison each polar pass is placed in one of four categories:

nominal—the baseline correction and choice of endpoints was done properly, no “eyeball” correction would improve the results significantly. Note that this does not necessarily mean that the data are good, there is still the possibility that the pattern changed during the pass, thus giving a confused or garbled result. “Nominal” means that, given the data for this particular pass, this analysis is probably as good as it will ever be.

bad—cases where the program has incorrectly chosen an endpoint in either the “H+ fuzz” or the auroral region, resulting in a skewed baseline and an erroneous potential curve.

data gap—throughout the DMSP data stream there are data gaps ranging from one minute to hours. In some cases where the gap is only a minute or two in length or else occurs outside of the polar auroral region it is possible to recover the potential curve for that pass. However, this is only done using the program DMSPDBASEINDV which requires a human in the loop to decide whether the pass is doable or not. For the automatic routines, neither DMSPDBASE2 nor DMSPDBASE3 has the sophistication to recover these passes. As a result the pass with the data gap returns a null file to the database and the subsequent pass is skipped over. Since such gaps are relatively infrequent (here < 2%) this is not considered a major flaw in the program.

failure—a case where the new algorithm has examined the data from 65 to 20 degrees magnetic latitude on both sides of the pass using steps of one degree and was unable to locate

either a suitable starting or stopping endpoint. Because this is part of the new algorithm, this case does not exist for the analysis using the old algorithm.

Using the data from March 1–10, 1988 (day 61–70) the old and new algorithms give the following results:

Using DMSPDBASE2 :

North: nominal 12 (9%) bad 120 (89.5%) data gap 2 (1.5%)

South: nominal 131 (98.5%) bad 0 (0%) data gap 2 (1.5%)

Using DMSPDBASE3:

North: nominal 128 (95.5%) bad 1 (0.7%) data gap 2 (1.5%) failure 3 (2.3%)

South: nominal 131 (98.5%) bad 0 (0%) data gap 2 (1.5%) failure 0 (0%)

Obviously, the new algorithm vastly improved the analysis on northern passes where the H+ fuzz was a problem. The two algorithms gave identical results in the southern hemisphere where the H+ fuzz was absent.

3.5 DMSPDBASE4—Upgrading the Heppner–Maynard Model Identification and Further Corrections to the Endpoint Selection Routine

From the summer of 1992 through December 1992 work was done on the latest version of the program which was called DMSPDBASE4. Two major problems were addressed in this revision. The first was a major improvement of the algorithm for classifying which Heppner–Maynard high latitude convection pattern a given pass matched. From this match an accurate value for the cross–cap potential could be determined. Thus the accuracy of the algorithm output is improved. This new algorithm was also generalized to work for all orbital orientations, not just the dawn–dusk orientation of F8. The second revision was a further refinement of the endpoint selection procedure to correct for the higher latitude endpoints on the dayside for the non–dawn–dusk oriented orbits. The code for the program was delivered to Phillips Laboratory/Geophysics Directorate in January 1993.

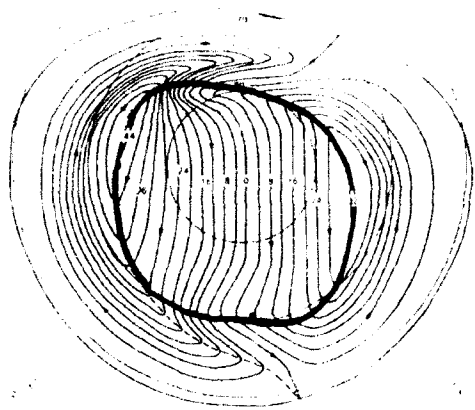
In the original DMSPOTMOD program each pass was analyzed to determine which of the three Heppner–Maynard models it most closely matched. The algorithm for this was a simplistic one. It assumed that the satellite travelled *only* exactly along the 0600–1800 hour meridian in the magnetic latitude/magnetic local time (MLT) coordinate system, then compared the asymmetry in the location of zero potential point along that line in the three models to the asymmetry seen along the spacecraft's track. The first failing of this algorithm comes from the fact that the F8 satellite does not travel exactly along this line for most of its orbits during a day. Because of the tilt of the magnetic dipole axis relative to the Earth's rotation axis, the track of the F8 satellite in magnetic latitude/MLT coordinates "wanders" between the nightside and the 0600–1800 MLT meridian over the course of a day in the northern hemisphere. In the southern hemisphere, the ground track "wanders" between the 0600–1800 MLT meridian and the dayside over the course of a day. Thus the difference between the asymmetry seen in a model along the 0600–1800 MLT meridian and the asymmetry seen by the satellite moving parallel to the 0600–1800 MLT meridian but 15 degrees away from it towards the nightside may be significant. The second failing of this algorithm comes from the fact that it does not take into account the orientation of the satellite. It assumes the satellite is travelling on the 0600–1800 MLT orientation, but none of the DMSP satellites after F8 flew in such an orientation. Thus the application of algorithm to F9, which flew in a 1000–2200 MLT orientation, surely gave inaccurate classifications of the Heppner–Maynard patterns for a significant fraction of the passes.

The offset of the satellite track from a purely 0600–1800 MLT line was recognized in the original DMSPOTMOD program when the program calculated the true cross–cap potential drop based on the observed potential maximum and minimum. Since it is unlikely that on any given pass the satellite will encounter the absolute maximum and the absolute minimum potential, the algorithm must somehow scale the observed maximum and minimum to get the cross–cap potential. The original DMSPOTMOD program attempted this, but only in an oversimplified manner. The program determined the highest magnetic latitude reached by the satellite on a given pass, then used that to denote one of only four correction factors (PSICORFAC) that were multiplied to the observed potential drop to get the "true" potential drop. If the pass went above 85 degrees, then it assumed that the observed

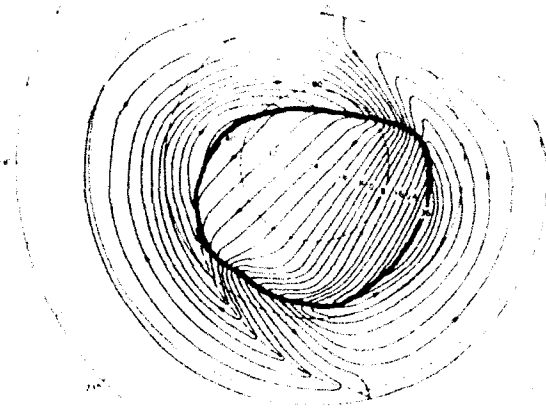
maximum and minimum were the true absolute maximum and minimum, so the correction factor was 1.000. If the highest magnetic latitude the satellite reached was between 80 and 85 degrees, then the correction factor was 1.085. If the highest magnetic latitude the satellite reached was between 75 and 80 degrees, then the correction factor was 1.215. If the pass failed to get above 75 degrees magnetic latitude, then it was assumed that the satellite failed to go through enough of the pattern to get a meaningful measurement, and so that pass was discarded and the correction factor was set to zero. The quantitative values of these correction factors were based empirically on the Heppner–Maynard models. The shortcoming of this algorithm was based on two factors, first that there were only three possible correction factors (along with the fourth indicating a discarded pass) instead of a varying range of possible correction factors, and second, that it was based only on the dawn–dusk orbital orientation of F8. Any other orbital orientation required a completely different set of correction factors. As the total cross–cap potential drop as well and the values of the absolute maximum and minimum potential are important inputs to the Magnetospheric Specification and Forecast Model (MSFM) program being run by the Air Weather Service, an upgrade of this algorithm was required. To correct for this, the algorithm was redone to map the location of the zero potential line relative to the convection reversal boundary and the potential distribution around the boundary for all three models. It had to compensate for the actual track of the satellite across the pattern and use that to match the pass to one of the models. In DMSPPOTMOD through DMSPDBASE3 the model matching and correction factor analysis were done in Blocks 3F and 3G, respectively. In the revision DMSPDBASE4 the analysis is combined into a single block now referred to as Block 3F/G. In the original program there were only four possible model classifications: 1 for model BC, 2 for model A, 3 for model DE, and 4 for unusable pass (probably northward IMF case). There are still only the three Heppner–Maynard models, but the new algorithm allows us to sort the unusable passes into several new categories. For example, in the original algorithm, any pass in which the observed potential difference between the maximum and minimum was less than 40 kV was classified as a 4. The rationale behind this was that such a small drop only occurred during times of northward IMF. However from the experience gained by analyzing the DMSP data, it was discovered that if only the magnitude of the

potential drop was known, there were at least three possible cases here: 1) The satellite passed close enough to the pole so that it did likely measure values close to the true potential maximum and minimum, and thus the low potential drop indicated this was indeed a northward IMF case. 2) The satellite passed close to the edge of the convection reversal boundary which indicated that the true potential drop may be larger than 40 kV, but the observed drop was less than 40 kV. Such passes may be actually be southward IMF cases corresponding to one of the three Heppner – Maynard patterns. 3) The satellite skimmed by the edge of the auroral zone and never passed through enough of the polar region to get a valid measurement. Such passes are referred to as “skimmers” and no information about the cross-cap potential and the IMF can be obtained from them. Reanalyzing the data using this revised algorithm allows us to differentiate between the true northward IMF cases and the cases of merely incomplete data. Also, a few of the cases that were originally classified as type 4 can now be reclassified as actually one of the three Heppner – Maynard patterns.

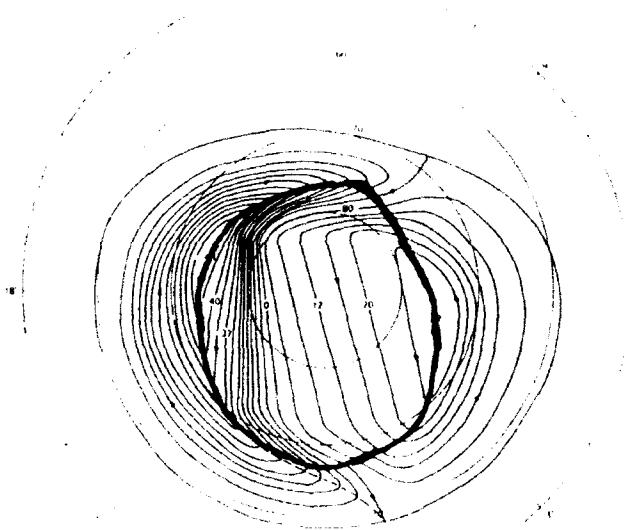
The algorithm starts by weeding out the easily identifiable passes. Any pass with a potential drop of less than 10 kV is identified as a skimmer and the model number (IMODNUM) is set to 5. This is based on the observation that even during northward IMF cases where the satellite passes close to the pole, the observed potential drop is something larger than 10 kV. Next the pass is checked to see if either the observed maximum or minimum potential is equal to zero. If this is true, then the pass covered a region of only positive or negative potential, and thus there is no way to determine which of the patterns it matches. This most often occurs on F9 and F10 when the satellite passes through only the negative potential region. For this case the model number is set to 6. Next it examines the pass to see if it went above 75 degree magnetic latitude but still had a potential drop of less than 40 kV. If this is true, then this is definitely a case of northward IMF and the model number is set to 4. If any of the above three cases are found to be true, then the program branches to the end of the block and continue on with the rest of the program. At this point all the passes that are not weeded out are eligible to be classified as one of the three Heppner – Maynard patterns (Figure 5) and the program can now move on to the pattern analysis. Some of the passes here will still prove to be unusable, but that will be taken care of at the end of the pattern analysis procedure.



(a)



(b)



(c)

Figure 5. These are the three Heppner–Maynard patterns for the electrostatic potential distribution in the polar ionosphere (*Heppner and Maynard, 1987*). This figure shows model A (a), model BC (b), and model DE (c). The convection reversal boundary has been highlighted on all three patterns. Note that because of the Harang discontinuity there is some ambiguity as to the exact location of the boundary in the region of 2100 to 0000 magnetic local time.

There are still some simplifications in the revised algorithm as a full pattern recognition algorithm based on a single pass is beyond the scope of this program at this time. The most significant simplification is that we treat the convection reversal boundary as a circle. While the true boundary is not a perfect circle, either in reality or in any of the three Heppner–Maynard models (see Figure 5), using a circle serves as a good approximation and simplifies the analysis procedure. We started by defining the convection reversal boundary and its center point for each of the three Heppner–Maynard models. We then mapped the zero crossing line as a function of angle and fraction of distance from the center point to the boundary at that angle. These measurements were then plotted onto a circle which gave us the three slightly distorted Heppner–Maynard zero potential line patterns shown in Figure 6. To determine which of the three models best fits the observations from a given pass, we must first figure out what the orientation of the pass was relative to the patterns and where the pass crossed the convection reversal boundary. We assume that the locations of the maximum and minimum potentials on a pass correspond to the convection reversal boundary and we convert their positions from magnetic latitude/MLT to x and y coordinates with the x,y origin set at the center of the magnetic latitude/MLT system (i.e.—at 90 degrees magnetic latitude). We assume for this analysis that the convection reversal boundary is a perfect circle that is centered near, but not necessarily at, the coordinate origin. Since there are only two points known here (the maximum and minimum locations) there are an infinite number of circles which contain both these points on their circumference. To choose a single circle we make a second simplifying assumption: that the radius of the circle is equal to the average of the distances between each extrema point and the coordinate origin. Again, this is not exact, but in most cases it gives a good approximation of the true location of the convection reversal boundary. With the radius of the circle given and the locations of the maximum and minimum known, we have narrowed down the location of the center of the circle to only two points. The algorithm calculates the locations of those two points in x,y coordinates, then selects the one closest to the coordinate origin to be the center of the circle.

With the radius and location of the center of the model convection reversal boundary determined, the program converts the locations of the observed maximum, minimum, and zero potential into the

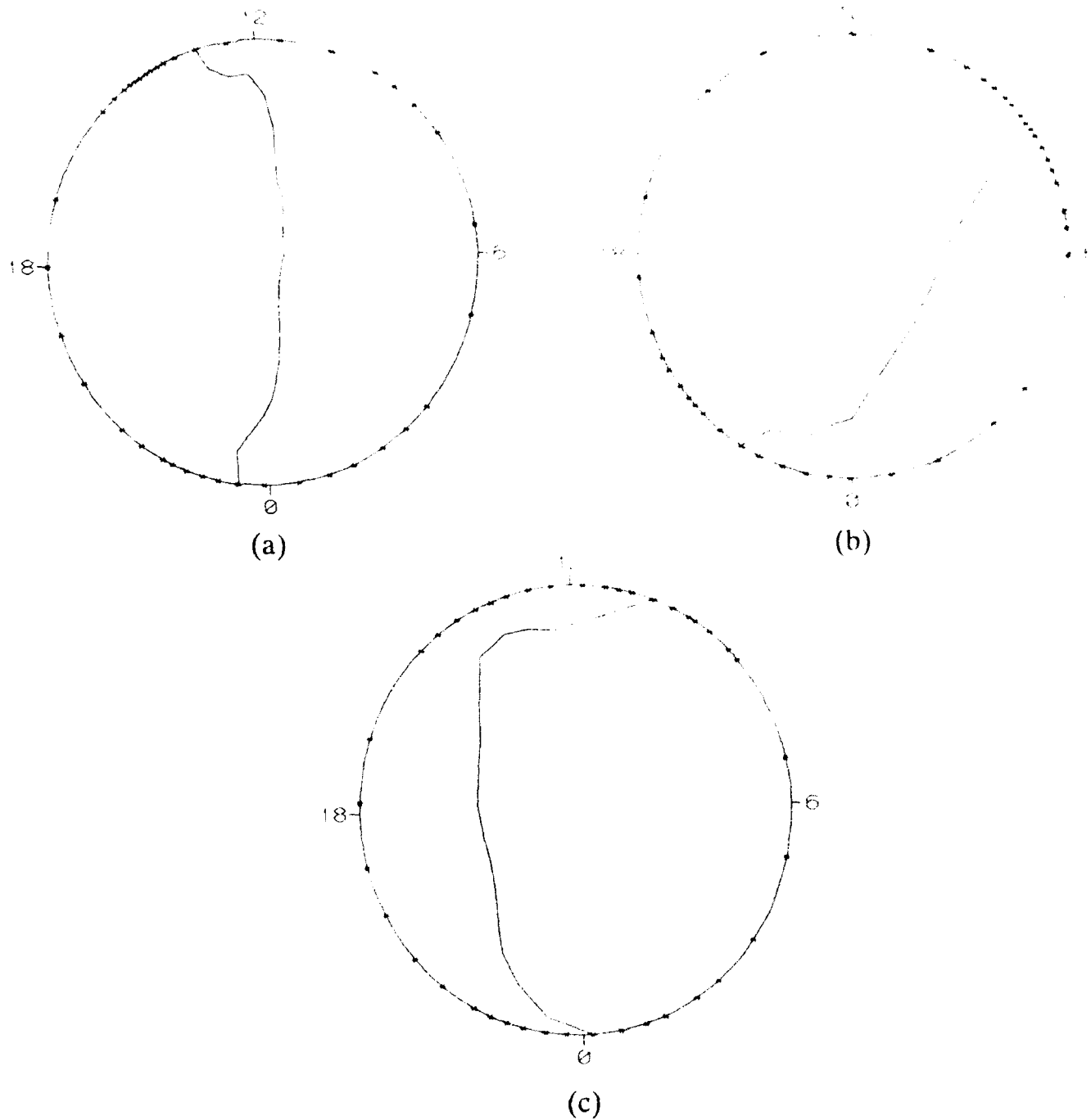


Figure 6. These patterns show the simplified convection reversal boundary and the zero potential line used in the program to identify the Heppner-Maynard model A (a), model BC (b), and model DE (c). These patterns have been distorted slightly relative to the true patterns shown in figure 5 by forcing the boundary to be a true circle. The asterisks on the boundary denote the potential distribution along the boundary in steps of 4 kV.

new coordinate system where the center of the circle is the origin. It then calls three subroutines (MODEL, MODELBC, and MODELDE) to calculate the location of the zero potential point along the satellite's track and the correction factors for the maximum and minimum potentials for each of the three Heppner–Maynard models. Each of these subroutines has only the data arrays for that specific model and that it then calls a further subroutine named MODEL to do the actual work. This allows for future models to be easily inserted into the program by simply adding another subroutine (say MODELFG) that contains only the data arrays to specify the potential distribution around the convection reversal boundary and the location of the zero potential line for that model. The location of the observed zero potential point along the track is used to calculate the distance between it and the location of the maximum. That distance is divided by the calculated length of the chord between the locations of the maximum and minimum potential to get the fractional distance called FRACORIG. The program then takes the returned locations of the zero potential point for each of the three Heppner–Maynard models, then calculates their fractional distances along the chord of the satellite track (FRACA, FRACBC, and FRACDE). Finally the program chooses the model with the fractional distance that is closest to the observed fractional distance as the model that best fits this pass. The program sets the model number to 1 for pattern BC, 2 for pattern A, and 3 for pattern DE, which are the same numbers used in the original DMSPPOTMOD program. At this point the program can weed out some of the ambiguous or distorted passes. Examination of the patterns in Figure 6 show that for almost every possible orientation of the satellite track, the smallest fractional distance from the observed maximum to the observed zero potential point always belongs to model BC and the largest always belongs to model DE. Only in two regions does this rule fail. On the dayside between 0900 and 1300 MLT and below 60 degrees magnetic latitude the location of the zero lines in model A and model DE trade places. On the nightside near 0000 MLT and at magnetic latitudes less than 60 degrees, zero potential lines get so close together that it become impossible to determine unambiguously which of the three models is the best fit. If the track of the satellite is such that it intersects either of these regions then the returned values for the fractional distances from the three models fail to meet the

FRACBC < FRACA < FRACDE condition. For those cases no determination can be made unambiguously, so those cases are ruled as unusable and the model number is set to 4.

When the MODEL A, MODEL BC, and MODEL DE subroutines are called they each return two correction values. These corrections are the numbers which are multiplied to the observed magnitudes of the potential maximum and minimum to get the absolute potential maximum and minimum for that model. These correction factors are calculated by taking the potential distribution around the convection boundary for the given model and comparing the potential at the location of the observed maximum (minimum) to the absolute maximum (minimum) for that model. When the program chooses the best fit model, then the correction factors for that model are set to the variables CORRECTMAX and CORRECTMIN. For the northward IMF, skimmer, and other unusable passes, the values of CORRECTMAX and CORRECTMIN are set to zero. The greater the distance between the location of the observed maximum (minimum) and the location of the absolute maximum (minimum) in the model, the larger the correction is going to be and the less certainty such a correction carries. For example, an observed maximum of 65 kV near 0700 MLT with a correction factor of 1.14 is obviously more certain than an observed maximum of 7 kV at 1030 MLT with a correction value of 10.57. While we cannot at this time give any quantitative reliability to these correction factors (other than the general caveat that the larger the correction, the more wary the investigator should be about using it) we have set a value of 10 for the cutoff for the correction factors. Any pass that ends up with a correction factor of 10 or more is ruled unusable and the model number is set to 7 and the values of CORRECTMAX and CORRECTMIN are set to zero. Also, there are a few cases where the real pattern is so distorted that the observed maximum (minimum) occurs in a region of the boundary which the model designates as negative (positive) and thus returns a negative value for the correction factor. Such a case is too distorted to be used and is also classified with a model number of 7. This gives us a total of eight possible categories for classifying each pass. The eight categories are summarized in the table below.

Table of model numbers for DMSPDBASE4

- 0*northward IMF (delta PSI < 40 kV, highest magnetic latitude point > 75 degrees)
- 1 HM model BC \
- 2 HM model A |—determined from model fitting subroutines
- 3 HM model DE /
- 4 unusable (zero occurred in far nightside or else pattern too distorted to classify unambiguously)
- 5 skimmer (unusable—delta PSI < 10 kV)
- 6 unusable (either observed maximum or minimum was zero)
- 7 unusable (one of the corrections greater than 10 or negative, pattern likely too distorted to classify unambiguously)

*Note that for null passes the value for the model is also set to zero. However these cases are easily distinguished from the northward IMF cases in that null passes have zero values for *all* the parameters.

We have compared the model classification results of two sets of ten-day periods of F8 and F10 data using the original DMSPPOTMOD through DMSPDBASE3 algorithm to the new model classification results using DMSPDBASE4 and summarized the results in the tables below. Note that for F8, there is not much change between the number of passes classified as a Heppner – Maynard pattern BC (model 1) and pattern DE (model 3) between the two algorithms. About half of the passes originally classified as pattern A (model 2) were reclassified as being pattern BC. As the original method assumed an F8 pass on a nearly dawn – dusk track, the fact that the old algorithm performed fairly well on F8 data is not surprising.

F8 1–10 January 1989

orig	# of passes	new 0	new 1	new 2	new 3	new 4	new 5	new 6	new 7	null
1	68	3	51	2	1	5	0	2	4	—
2	33	3	14	12	1	2	0	0	1	—
3	4	0	0	1	3	0	0	0	0	—
4	157	69	10	1	0	11	43	21	4	—
null	13	3	1	0	0	0	1	0	0	8
total	277	78	76	16	5	18	44	23	9	8

F8 1–10 April 1989

orig	# of passes	new 0	new 1	new 2	new 3	new 4	new 5	new 6	new 7	null
1	104	1	81	4	0	10	0	6	2	—
2	76	2	32	36	1	3	0	0	2	—

3	6	0	0	1	5	0	0	0	0	—
4	87	32	3	1	2	9	28	10	2	—
null	3	0	2	1	0	0	0	0	0	0
total	276	35	118	43	8	22	28	16	6	0

The next two tables show the results of the new algorithm on two sets of F10 data. Since F10 is in a 0800–2000 MLT orbit the original algorithm did not perform as well as it did for F8. After using the new analysis only about 45% of the passes originally classified as pattern BC (model 1) remain as pattern BC, while about 25% are reclassified as pattern A (model 2) and the remainder fall into one of the non–Heppner–Maynard categories. There was less change seen in the pattern A (model 2) passes. Just over 60% of the passes originally classified as pattern A remained in that category after the new analysis, while about 8% were reclassified as pattern BC, and about 10% were reclassified as pattern DE (model 3). Overall only around one–third of the F10 passes fall into one of the three Heppner–Maynard patterns compared to nearly one–half of the F8 passes, while the percentage of “unsuitable passes” (model numbers 4–7) increased from 30% for F8 to 38% for F10. This is likely a result of the different orbital orientation of the F10 spacecraft relative to F8.

F10 1–10 January 1991

orig	# of passes	new 0	new 1	new 2	new 3	new 4	new 5	new 6	new 7	null
1	33	3	15	9	0	3	0	1	2	—
2	24	0	1	15	5	0	0	0	3	—
3	13	0	0	2	10	1	0	0	0	—
4	153	77	3	6	1	19	38	7	2	—
null	26	4	3	2	3	3	4	1	2	4
total	249	84	22	34	19	26	42	9	9	4

F10 1–10 April 1991

orig	# of passes	new 0	new 1	new 2	new 3	new 4	new 5	new 6	new 7	null
1	76	2	34	18	0	3	0	17	2	—

2	24	0	3	14	0	1	0	0	6	
3	9	0	0	1	5	2	0	0	1	
4	93	34	1	1	1	28	3	24	1	
null	42	7	5	5	1	6	3	7	0	8
total	244	43	43	39	7	40	6	48	10	8

An additional benefit of the new algorithm can be seen in the fact that a large number of the passes originally classified as "null passes" under the old algorithm turn out to be analyzable passes under the new algorithm, although about half of them still end up classified in one of the "unsuitable passes" categories. This is particularly dramatic in the two F10 tables where over 80% of the "null passes" under the old algorithm become good passes under the new algorithm. This raises the percentage of analyzable passes for the two ten-day periods of F10 from the 80% range to the 90% range.

The requirement that the potential correction factors be saved to the database along with the re-doing of the model number classification scheme meant that we had to reformat the shortfile. To keep the size of the 128 character record per pass constant we had to delete something to make room for the correction factors. The value of the average of the potential maximum and minimum (POTMEANSF) and the location where it occurred (POTMEANMLT and IPOTMEANMLAT) had not proven to be a useful parameter. Furthermore, since the entire set of potentials for a given pass were being saved in the longfile, these values could be easily recovered if the need ever arose. These three values were replaced with the two correction values (CORRECTMAX and CORRECTMIN) and the highest magnetic latitude the satellite reached on this pass (MLATHIGH). As with the other magnetic latitudes in the shortfile, the value saved is the latitude times ten in order to remove the need for the decimal point. This variable will enable investigators to easily ascertain the degree to which any given pass penetrated the polar cap region.

IQUALFLAG is now a only 2-digit integer, but still formatted as I4 as in the original shortfile. The hundreds place was the IPSICORFAC (PSI CORrection FACTor) variable, which no longer exists since it is now superseded by the new CORRECTMAX and CORRECTMIN variables. The tens

place is still IQFLAG (Quality FLAG) which is unchanged from the original shortfile. The final digit is the model number (IMODNUM) classification discussed above and now ranges from 0 to 7.

The two data file formats for the shortfile are given below (the * indicates a change between the two):

OLD SHORTFILE FORMAT			NEW SHORTFILE FORMAT		
item	format		item	format	
SFINDEX	A12		SFINDEX	A12	
PSIMAXSF	F5.1		PSIMAXSF	F5.1	
SCMLTMAX	F5.1		SCMLTMAX	F5.1	
INVLATMAX	I5		INVLATMAX	I5	
IMLATMAX	I5		IMLATMAX	I5	
PSIMINSF	F7.1		PSIMINSF	F7.1	
SCMLTMIN	F5.1		SCMLTMIN	F5.1	
INVLATMIN	I5		INVLATMIN	I5	
IMLATMIN	I5		IMLATMIN	I5	
IQUALFLAG	I4	*	IQUALFLAG	I4	
ZEROMLT	F5.1		ZEROMLT	F5.1	
IZEROMLAT	I5		IZEROMLAT	I5	
PLMIDPOTSF	F7.1		PLMIDPOTSF	F7.1	
PLMIDMLT	F5.1		PLMIDMLT	F5.1	
IPLMIDMLAT	I5		IPLMIDMLAT	I5	
POTMEANSF	F7.1	*	CORRECTMAX	F6.3	
POTMEANMLT	F5.1	*	CORRECTMIN	F6.3	
IPOTMEANMLAT	I5	*	MLATHIGH	I5	
KPSHORT	I3		KPSHORT	I3	
IAEINDEX	I4		IAEINDEX	I4	
BXSHORT	F5.1		BXSHORT	F5.1	
BYSHORT	F5.1		BYSHORT	F5.1	
BZSHORT	F5.1		BZSHORT	F5.1	
IPOTOFF	I4		IPOTOFF	I4	

Total 24 columns 128 characters plus one 0x0a code (a linefeed at the beginning of each line), forming 129 bytes/record.

The second major revision in DMSPDBASE4 is a further refinement of the endpoint selection algorithm. As was explained above, the revised algorithm in DMSPDBASE2 began looking for each endpoint by examining the data at 65, 60, 55, and 50 degrees magnetic latitude and if more than one was acceptable, it choose the one that was the lowest in latitude. This choice was based on the assump-

tion that if a higher latitude point was also acceptable, then the potential drop between the higher and lower latitude points was zero, and that extending the "tail" of the potential curve at either end would only result in a flat line at essentially zero potential. For most cases this assumption held, as can be seen in Figure 7 where the potential is essentially zero from 50 degrees to 60 degrees magnetic latitude on the dawnside (left side of graph) and from around 57 degrees to 50 degrees on the duskside. The preference of 50 degrees magnetic latitude as a starting and ending latitude was historical in its basis. Fifty degrees as a nominal and safe choice for the zero potential was used throughout all the earlier work on NASA's Dynamics Explorer. Most of the concern had been on making the algorithm robust enough to handle cases when the polar cap boundary expanded during storm periods where the starting and stopping endpoints had to be reset equatorward of the 50 degree line. However as the analysis progressed there were some occasions where a combination of a small polar cap boundary combined with differences in the flow baseline on either side of the pass would result in a false potential trough or hump appearing equatorward of the auroral region. Figure 8 shows an example of this on the dusk-side (right side) of the potential curve. The slight difference in the baselines in the horizontal flow on either side of the polar region would not make very much difference if the endpoints were just equatorward of the auroral regions. But the slight offset of the flow during the six minute period from minute 46 through minute 52 (roughly 65 degrees magnetic latitude to 50 degrees) results in a shallow basin of negative potential in the corrected potential curve. Since this occurs on the dawnside of a track that is almost exactly along the 0600–1800 line, this portion of the potential should normally be either positive or zero, and thus this negative potential basin is clearly an artifact of the processing procedure. While this occurred infrequently in the F8 data, it appeared more often in the F9 and F10 data. The region of zero potential reaches to higher latitudes on the dayside than on the nightside or on the dawn–dusk line, thus the tilt of these satellites' orbits away from the dawn–dusk orientation of F8 causes them to observe zero flows (i.e.—zero potential) on the dayside at higher latitudes than observed by F8. These artifacts interfere with the accuracy of electric field modelling routine in the MSFM, and this was brought to our attention by the personnel from Rice University at the Quarterly Review Meeting held in Colorado Springs in November 1992 (see Freeman et al., 1992). The MSFM

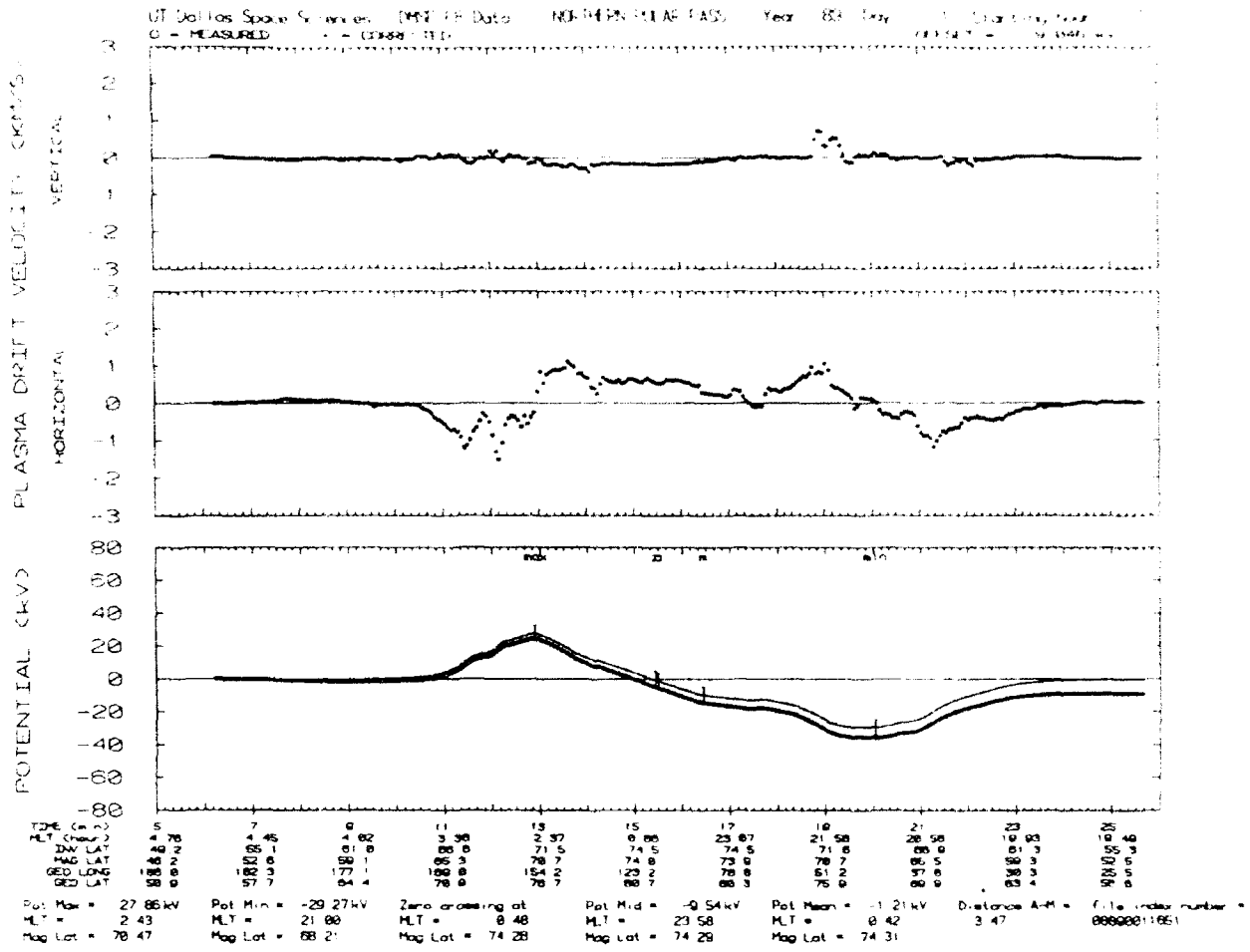


Figure 7. This is a plot of a pass where there is a large amount of near-zero flow between 50 and 60 degrees on both sides of the polar region. Note that these "tails" have little effect on the potential curve calculated and shown in the bottom panel.

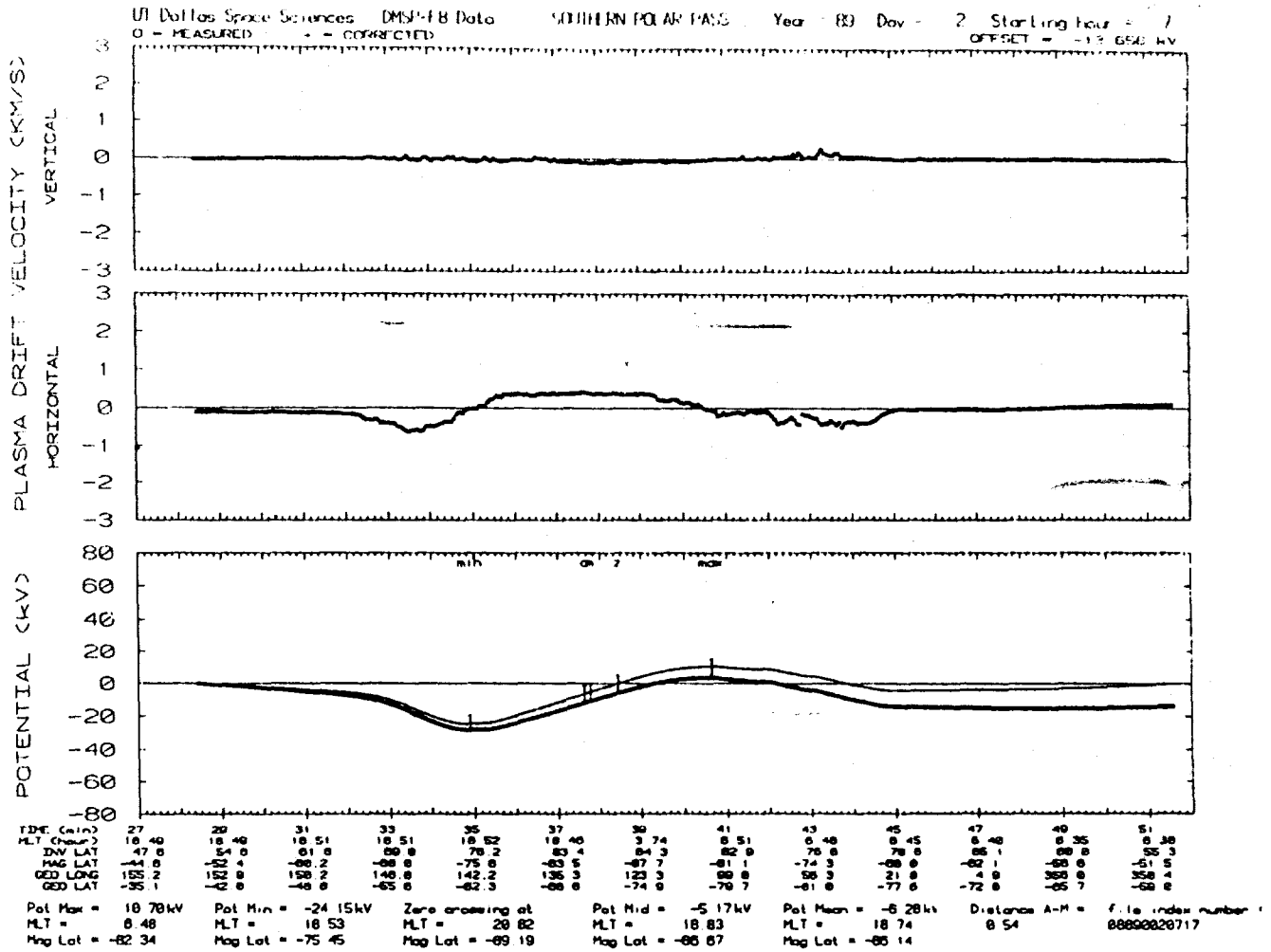


Figure 8. This pass is similar to the one in figure 7, except that the flow equatorward of the auroral region is does not go to zero. Since there is a difference in the baseline determined by the flow on the duskside (left) and the dawnside (right), the program averages the difference and comes up with a baseline that gives non-zero flows on either side. This small, but non-zero flow in these "tails" results in an artificial negative potential region on the dawnside between the auroral region and 50 degrees.

attempts to fit a potential curve to the erroneous portion of a potential curve such as shown in Figure 8 which obviously degrades the ability of the MSFM to produce quality results. At their request we began to redo the algorithm to take care of these artifacts. Initially there was some concern that any change that would push the endpoint towards higher latitudes for these problem passes, might inadvertently degrade the quality of the analysis of the nominal passes. By pushing the endpoints of nominal passes to higher latitudes this might change the baselines which would change the calculated potentials, or it might even accidentally push the endpoints into the polar region and miss the auroral portion of the pass altogether.

Fortunately, the fix turned out to be quite simple and caused little or no perturbation of the data for the nominal passes. The revised algorithm gets rid of the 50 degree preference by simply starting the check procedure of the data at 65 degrees magnetic latitude and proceeding equatorward in five degree steps until either an acceptable endpoint or 20 degrees is reached. This guarantees that the highest latitude point that is suitable is used as the endpoint for that end of the pass. Figure 9 shows the new potential for the pass shown in Figure 8 using this new algorithm to choose the endpoints. This time the pass starts at 60 degrees magnetic latitude and stops at 65 degrees. (Note that in this report and in the program we use only the absolute value of magnetic latitude for our analysis and descriptions. The negative sign on the magnetic latitude shown in the figure above merely indicates that the pass occurred in the southern hemisphere.) Note that this gets rid of the false negative potential region on the dawnside and resets the maximum and minimum potential values, probably closer to the true values than was the case in the first analysis. Figure 10 presents the same pass as was shown in Figure 7 after using the new algorithm. This results in only clipping the zero potential regions on either end. The corrected maximum and minimum potentials are changed by less than 2% from their values in the old analysis. While this new version decreases the likelihood of false potentials appearing in the data because of a bad choice of endpoints, it should be strongly emphasized that this routine is still not absolutely 100% foolproof. The level of confidence in all of this analysis must continually be reevaluated in light of the changing conditions of the data that the program faces. As we move

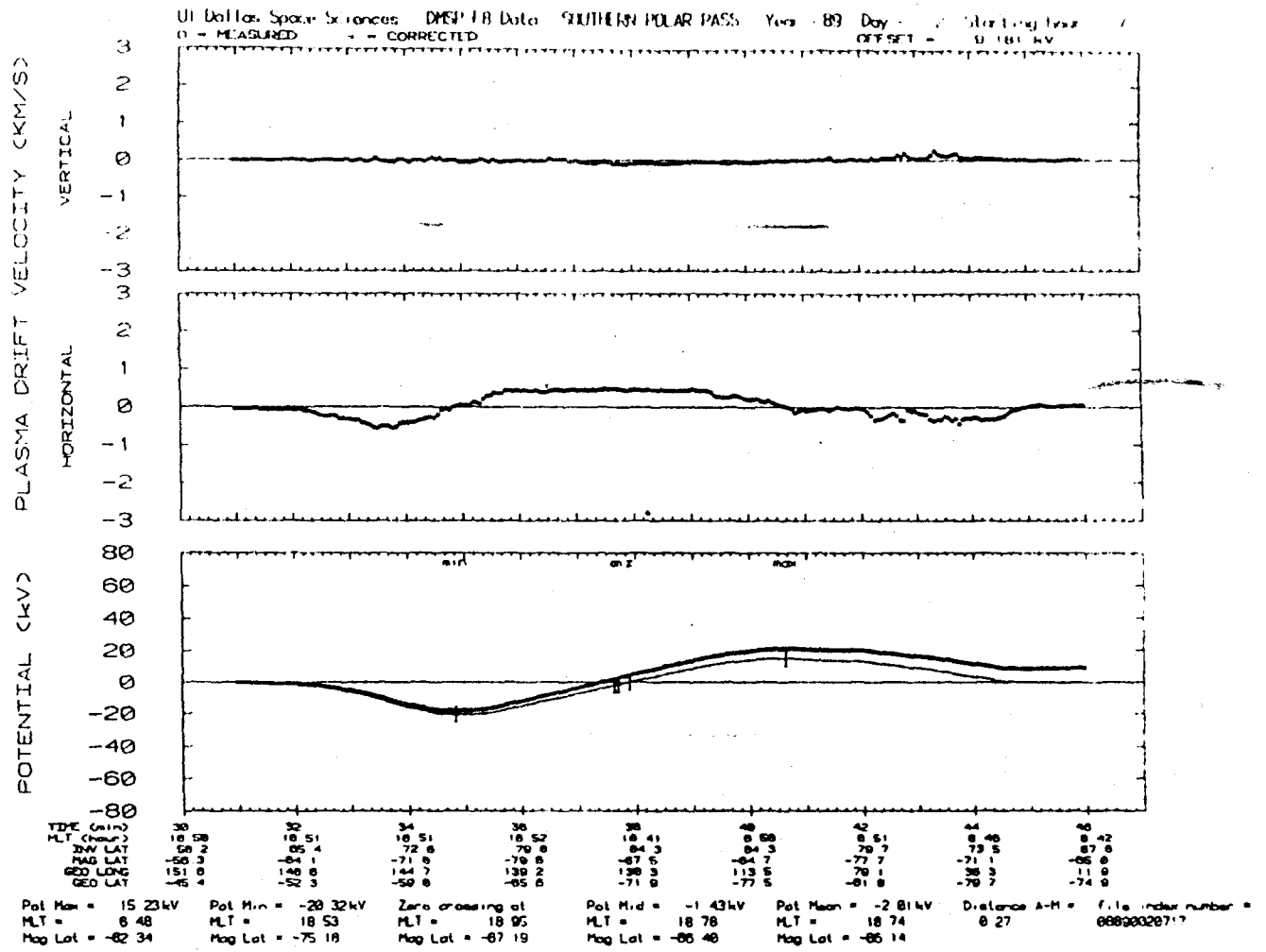


Figure 9. This is the same pass as in figure 8 except that the endpoints have been moved poleward to avoid including the non-zero "tails" in the flow in the potential calculations. Note that the artificial negative potential region has disappeared. Also the magnitudes of the maximum and minimum and location of the zero point have changed from figure 8.

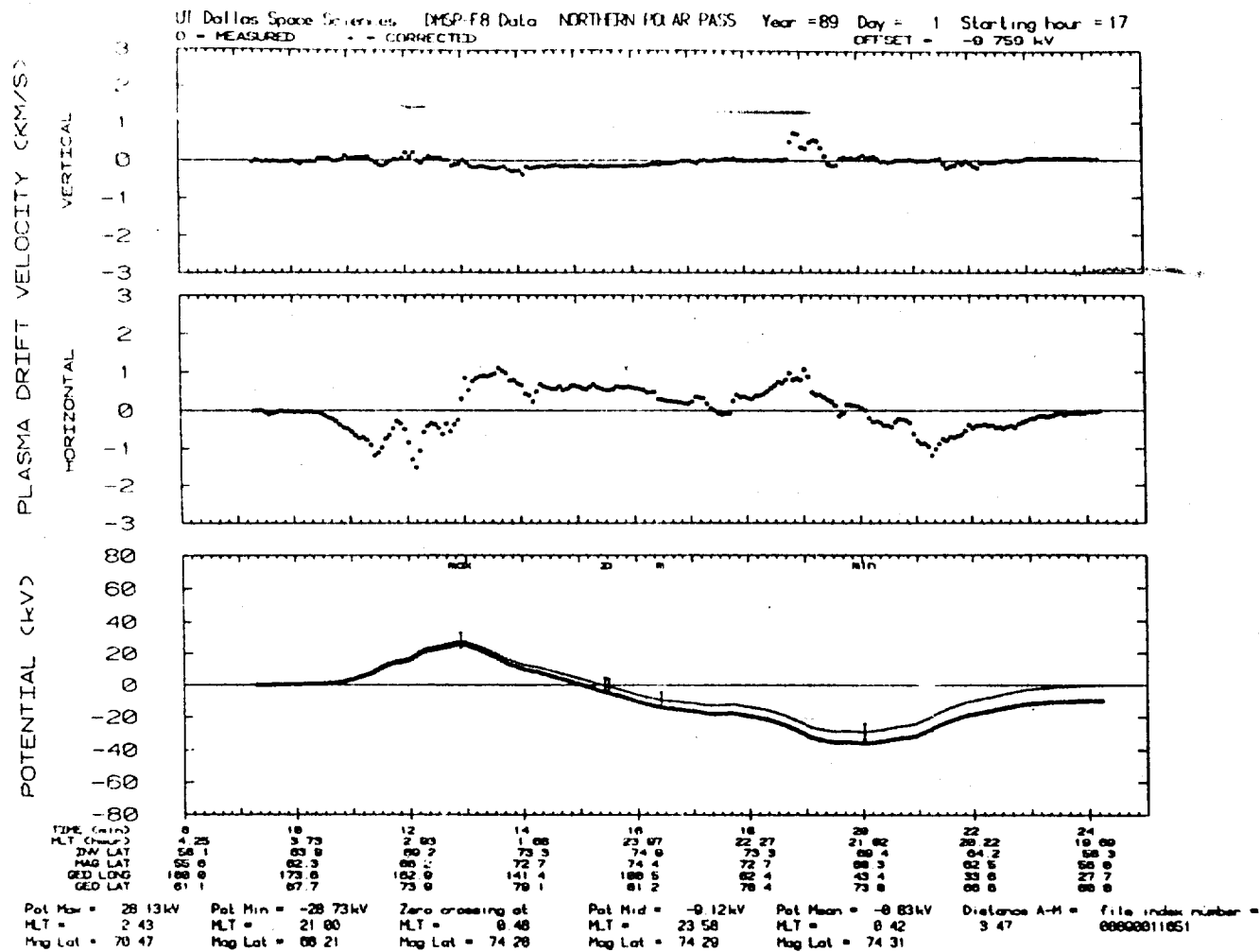


Figure 10. This is the same pass as in figure 7 except that the endpoints have been moved poleward to avoid including the near-zero "tails" in the potential calculation. Note that removing the "tails" has not significantly changed the locations or magnitudes of the maximum or minimum.

towards solar minimum, the ionospheric conditions will likely change and this may be reflected in the quality of the analysis, which in turn may require some further upgrades be made to DMSPDBASE4.

4. OTHER ANALYSIS EFFORTS

While most of the effort performed on this contract has been on upgrading and maintaining the analysis programs we have developed, we have devoted a fair amount of time to efforts using the data generated for the DMSP database. Our major focus has been on characterizing the convection patterns observed during times of steady IMF conditions when B_z is southward. With the continuous data stream from DMSP, we can use take extended times of steady IMF conditions to compare the patterns seen simultaneously in both polar region using multiple satellites. Generally we have found that the patterns seen are consistent with the Heppner–Maynard patterns, but we have been surprised to find that there is roughly a 10% difference between the total cross–cap potential drops observed in the two hemispheres. We are in the final stages of preparing a paper on our results of this study for submission to the *Journal of Geophysical Research*. In conjunction with this work we have developed a three–dimensional presentation of the data which allows the user to examine the magnitude and shape of the potential curve at the same time as the location of the satellite's track in the magnetic latitude/magnetic local time coordinate system is shown (Figure 11). This enables us to clearly present a larger set of data in a single figure without overwhelming the audience or reader. A short animation of the data using this technique was submitted on videotape to Phillips Lab in spring 1991.

Judy Cumnock, one of the graduate students here at the University of Texas at Dallas, has been concentrating on identifying flow patterns observed during times of extended northward IMF conditions. Her work studying the pattern during the January 14, 1988 period showed evidence of a two–cell pattern metamorphosing into a four–cell pattern as the IMF orientation rotates from predominantly B_y to predominantly $+B_z$. This work has been presented at an American Geophysical Union meeting and has been published in the *Journal of Geophysical Research* (Cumnock et al., 1992). She is expanding this work into a doctoral thesis which will examine more cases of convection patterns during northward IMF conditions for the 1988–1990 period. We currently have two other graduate students working on analysis of the DMSP data for their doctoral work. Chris Keating has worked on

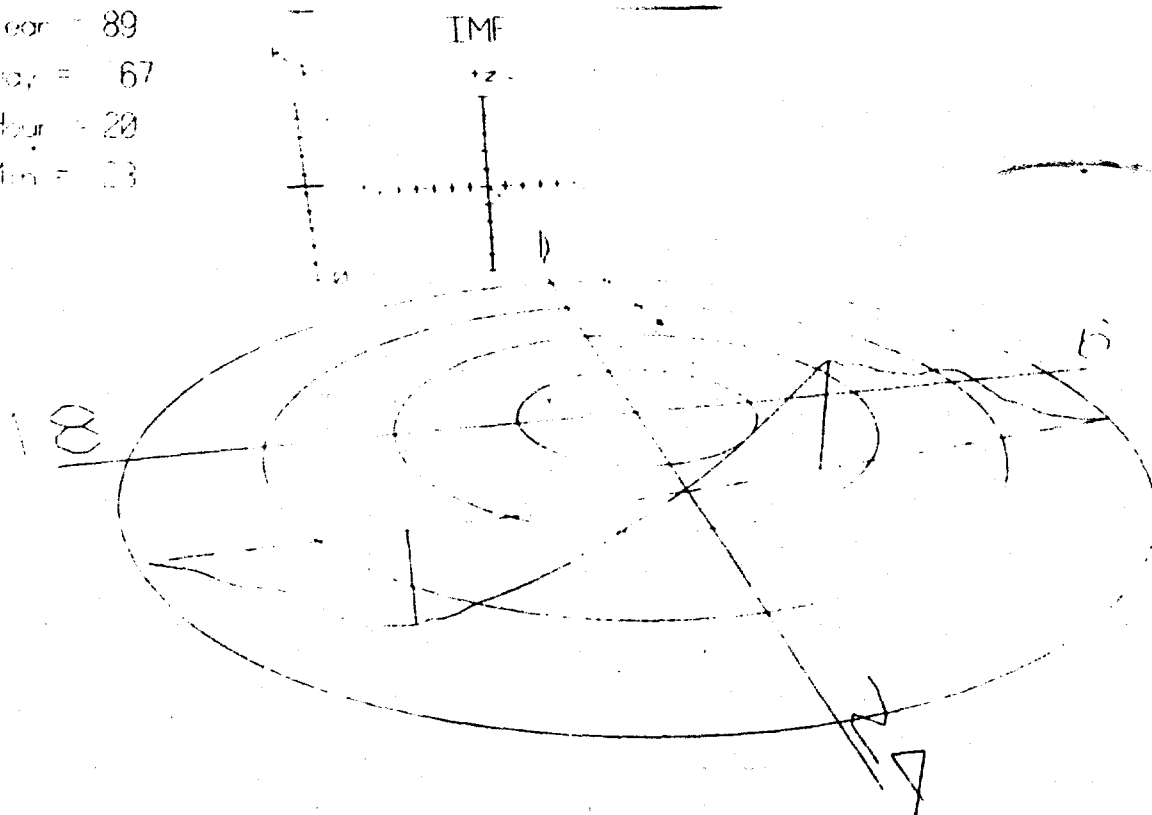
IMSP-F8 Northern Hemisphere

Year = 89

Day = 67

Hour = 20

Min = 23



08890671957

Figure 11. This is a three dimensional representation of a polar pass. The viewpoint is from the nightside looking towards the dayside. The ground track is represented by the dashed line on the dial. The potential is represented by the curve above (positive potential) and below (negative potential) the dashed line. The locations and magnitudes of the potential maximum and minimum are shown by the two vertical lines connecting the potential curve and the ground track. In front of the noon-midnight line are two glyphs. The one on the left is a sliding bar that shows the K_p value during the pass. The other glyph shows the orientation and magnitude of the IMF in the y-z plane. Note that this is oriented such as it would appear to an observer looking towards the sun from the Earth. Thus y is positive to the left and negative to the right. Here we show a case where B_z and B_y are both negative.

identifying periods when the orbits of DMSP-F8 and F9 were in phase with each other, then using the data from those passes to characterize the shape of the convection reversal boundary. Keith West just started this past year and is looking at equatorial data from DMSP, a portion of the database that we have generally ignored up to this point. Both Cumnock's and West's work on DMSP analysis have been funded by the Texas Space Grant Consortium.

A major portion of our effort in data analysis went into producing and providing usable DMSP data for several other investigators and other institutions. Feedback from these other groups has been invaluable in honing the computer analysis tools. As the software has matured, fulfilling these requests has become more routine and automated. However some of them still require special handling to produce, such as for cases where the user wants only data that was acquired only over certain geographic regions. We have provided data to the following individuals or groups:

* Major Delores Knipp at the US Air Force Academy. She has incorporated the measured potential from DMSP into the Assimilative Mapping of Ionospheric Electrodynamics (AMIE) routine to help in modelling the polar electric field.

* Drs. Richard Wolf and Robert Spiro at Rice University. They have developed the MSFM package for use by the Air Weather Service and much of our work described above on DMSPDBASE was motivated by the needs of the MSFM program.

* Dr. John Freeman and Akira Nagai at Rice University. They have been working on developing a neural network which will predict the future convection pattern in the polar ionosphere based on the previous several hours' observations. This work uses the shortfile output from DMSPDBASE as a testbed.

* Dr. Mark Loranc at Marshall Space Flight Center (formerly at the University of Western Ontario). He has been comparing the flow velocities observed by DMSP when it passes over the BARS radar site in Canada with the measured ion flows seen by the radar.

* Dr. Ennio Sanchez at Johns Hopkins Applied Physics Laboratory. He has used DMSP-F9 ion flow data to compare to and calibrate data from the PACE radars during substorms.

* Dr. David Knudsen at Max-Planck-Institut für extraterre Physik. He compares the DMSP data

with the radar data from the EISCAT radar.

*Dr. Geoff Crowley at Lowell University. He compares the DMSP flow with radar data in the cusp region.

*Drs. Barbara Emery and Gang Lu at the National Center for Atmospheric Studies (NCAR). They have used the ion flow from several of the DMSPs to do ionospheric modeling.

* Dr. Mervyn Freeman at the British Antarctic Survey. He and his colleagues used DMSP flow data to model the ionospheric polar convection pattern during specific times of northward IMF.

Much of this work, both here at UT Dallas and in collaboration with other groups, has been presented at meetings of the American Geophysical Union. Below is a list of the AGU presentations over the past three years which have dealt with DMSP data analysis covered in this contract. An asterisk indicates a presentation given by a member of the research group here. The final letter and number code after the title gives the AGU code number for that presentation.

AGU Spring 1990

none

AGU Fall 1990

*Hairston, M. R., R. A. Heelis, and F. J. Rich, Characterization of Ionospheric Flow Patterns in Northern and Southern Polar Regions Using DMSP Data SM12B-2

Knipp, D. J., B. A. Emery, A. D. Richmond, M. R. Hairston, R. A. Heelis, and F. J. Rich, Mapping Ionospheric Convection with Satellite Ion Drift Measurements SM12B-1

AGU Spring 1991

*Hairston, M. R., R. A. Heelis, and F. J. Rich, Comparison of Simultaneous Ionospheric Flow Patterns in Northern and Southern Polar Regions Using DMSP Data SA51B-4

Rich, F. J., W. J. Denig, M. R. Hairston, and R. A. Heelis, A Search for the Signature of Flux Transfer Events Near the Dayside Ionospheric Cusp SM42A-7

AGU Fall 1991

*Hairston, M. R., R. A. Heelis, and F. J. Rich, Ionospheric Polar Cap Potential Distribution for March 1989-- - The Movie SA12A-7

*Cumnock, J. A., R. A. Heelis, and M. R. Hairston, Ionospheric Observations of Sunward Convection at Very High Latitudes SA12A-9

AGU Spring 1992

Nagai, A., J. W. Freeman Jr., P. H. Reiff, R. A. Wolf, F. J. Rich, and M. R. Hairston, Short-term Forecast of Magnetospheric Parameters by a Neural Network System SM32A-3

AGU Fall 1992

Emery, B. A., A. D. Richmond, D. J. Knipp, M. R. Hairston, and W. F. Denig, Polar Ionospheric Electrodynamics and Energy Inputs in the Northern and Southern Hemispheres for a Strong Interplanetary Magnetic Field SA21B-2

Rich, F. J., M. S. Gussenhoven, and M. R. Hairston, DMSP Observation of Precipitating Particles and Electric Field During the GEM Campaign SM41B-4

Boyle, C. B., P. H. Reiff, A. Nagai, M. R. Hairston, and R. A. Heelis, DMSP Driven Estimates of Polar Cap Potential SM51A-1

Much of this work has been presented as research papers which are in various states of acceptance in the refereed literature. The list of papers is presented below:

Papers published

Cumnock, J. A., R. A. Heelis, and M. R. Hairston, Response of the ionospheric convection pattern to a rotation of the interplanetary magnetic field on January 14, 1988, *J. Geophys. Res.*, 97, 19449-19460, 1992.

Papers accepted and awaiting publication

Freeman, M. P., C. J. Farrugia, L. F. Burlaga, R. P. Lepping, M. E. Greenspan, J. M. Ruohoniemi, and M. R. Hairston, The interaction of a magnetic cloud with the Earth: Ionospheric convection in the

northern and southern hemispheres for a wide range of quasi-steady interplanetary magnetic field conditions, accepted by *J. Geophys. Res.* in 1992, to be published in 1995.

Papers submitted

Emery, B. A., D. J. Knipp, A. D. Richmond, N. U. Crooker, M. R. Hairston, et al., Ionospheric response to an interplanetary magnetic cloud -- I. Overview of analysis for 1988 January 14-15, submitted to *J. Geophys. Res.* 1992.

Knipp, D. J., B. A. Emery, A. D. Richmond, N. U. Crooker, R. A. Heelis, M. R. Hairston, J. A. Cumnock, et al., Ionospheric response to an interplanetary magnetic cloud -- II. A case study of 14 January 1988, submitted to *J. Geophys. Res.* 1992.

Rich, F. J. and M. R. Hairston, Large scale convection patterns observed by DMSP, submitted to *J. Geophys. Res.* 1992.

Papers in final stages awaiting submission

Hairston, M. R., R. A. Heelis, and F. J. Rich, Comparison of simultaneous potential distribution patterns in the northern and southern polar ionosphere, to be submitted to *J. Geophys. Res.* 1993.

References

- Cumnock, J. A., R. A. Heelis, and M. R. Hairston, Response of the ionospheric convection pattern to a rotation of the interplanetary magnetic field on January 14, 1988, *J. Geophys. Res.*, *97*, 19449–19460, 1992.
- Freeman, J. W., R. Wolf, R. Spiro, A. Nagai, R. Hilmer, and B. Hansman, Magnetospheric Specification and Forecast Model—Review Meeting, Peterson AFB, Colorado Springs, CO, November 11, 1992.
- Heelis, R. A., and M. R. Hairston, Studies of ionospheric dynamics utilizing data from DMSP, GL-TR-90-0047(I), Air Force Geophys. Lab., Hanscom AFB, MA, April 1990, ADA223370.
- Heppner, J. P., and N. C. Maynard, Empirical high-latitude electric field models, *J. Geophys. Res.*, *92*, 4467–4489, 1987.